HHS Public Access

Author manuscript

Sci Immunol. Author manuscript; available in PMC 2022 June 10.

Published in final edited form as:

Sci Immunol. 2021 December 10; 6(66): eabg0336. doi:10.1126/sciimmunol.abg0336.

Effective CD4 T Cell Priming Requires Repertoire Scanning by CD301b$^+$ Migratory cDC2 Cells upon Lymph Node Entry

Naoya Tatsumi[1,2], **Alicia L. Codrington**[1,2], **Jihad El-Fenej**[1,2], **Varoon Phondge**[1,2], **Yosuke Kumamoto**[1,2,*]

[1]Center for Immunity and Inflammation, Rutgers New Jersey Medical School, Newark, NJ 07103

[2]Department of Pathology, Immunology and Laboratory Medicine, Rutgers New Jersey Medical School, Newark, NJ 07103

Abstract

During the initiation of adaptive immune responses, millions of lymphocytes must be scanned to find the few cognate clones. The activation mechanisms of CD4 T cells have been extensively studied, but the cellular mechanisms that drive selection of cognate clones are not completely understood. Here, we show that recently homed naive polyclonal CD4 T cells are temporarily retained before leaving the lymph node. This stop-and-go traffic of CD4 T cells provides an adequate time window for efficient scanning and timely priming of antigen-specific cognate clones. CD301b$^+$DCs, a major subset of migratory cDC2 cells, localize to the areas around high endothelial venules, where they retain incoming polyclonal CD4 T cells through MHCII-dependent, but antigen-independent mechanisms, while concurrently providing cognate stimuli for priming. These results indicate that CD301b$^+$DCs function as an immunological “display window” for CD4 T cells to efficiently scan their antigen specificity.

One Sentence Summary:

CD301b$^+$ migratory cDC2 cells temporarily retain polyclonal CD4 T cells during priming to scan their antigen specificity

Introduction

Naive T cells undergo a multi-step activation process during the initiation of adaptive immune responses, including homing to the draining lymph node (dLN), transient interactions with conventional dendritic cells (cDCs), engagement with cDCs presenting cognate peptides, and rapid proliferation and differentiation (1–3). Antigen-specific T cell

*Corresponding author: yosuke.kumamoto@rutgers.edu.

Author contributions: N.T. and Y.K. designed experiments. N.T. performed most of the experiments with help from A.L.C., J.E-F and V.P. Y.K. designed the targeting constructs of the Mgl2-Cre and Itgax-dlDTR mice and performed initial characterization. N.T. and Y.K. analyzed and interpreted the data. N.T. performed statistical and computational analyses. Y.K. conceptualized and supervised the study and acquired funding. N.T. and Y.K. wrote the paper.

Competing interests: The authors declare no competing interests.

Data and materials availability: All raw data used for generating the graphs shown in the paper are available in Supplementary Materials. Mgl2-DTR and Mgl2-Cre mice are available upon request from Y.K. under material transfer agreement (MTA) from Yale University. CD11-dlDTR mice are available upon request from Y.K. under MTA from Rutgers University.

clones are extremely rare, so scanning for the antigen-specificity of polyclonal T cells must be highly efficient in order to combat invading pathogens in a timely manner. cDCs provide the most critical signal for T cell priming by presenting antigen-derived peptides, and they also provide structural support for maximizing T cell responses by inducing LN hypertrophy and recruiting polyclonal T cells to the dLN (4–6).

Naive mouse skin is populated with three major migratory DC subsets, including epidermal Langerhans cells, dermal CD103$^+$ DCs, and dermal CD301b$^+$ DCs, all of which continuously migrate from the skin to the dLN and preferentially induce T helper (Th) 17, Th1 and Th2 differentiation of antigen-specific CD4 T cells, respectively (7, 8). These migratory DCs had long been thought to be critical for initiating T cell responses against skin-borne antigens, but recent studies showed that dLN-resident DCs can initiate T cell responses before the arrival of the migratory subsets by directly acquiring antigens from the lymph, especially soluble antigens (9–11). It is well documented that different migratory DC subsets induce different types of Th cells, but their subset-specific roles in the initiation of CD4 T cell priming are poorly understood.

CD301b$^+$ DCs are a subset of type 2 cDC (cDC2) cells and account for the majority of migratory CD11b$^+$ cDCs in the dermis (12–14). Previous studies have shown that the differentiation of Th2 effector cells was selectively impaired when CD301b$^+$ DCs were absent or specifically depleted in Mgl2-DTR mice, which express the diphtheria toxin receptor (DTR) under the regulation of the *Mgl2* gene (encoding CD301b) (12, 14, 15). However, it remains unclear whether the role of CD301b$^+$ DCs is limited to the induction of Th2 fate, or if they also have a subset-specific role in CD4 T cell priming, such as scanning the antigen specificity of polyclonal CD4 T cells and triggering cell cycle entry of the cognate clones.

Here we demonstrate that CD301b$^+$DCs are required for effective priming of CD4 T cells, especially for rare antigen-specific clones. Newly homed naive polyclonal CD4 T cells in the dLN are temporarily retained by CD301b$^+$DCs in an MHCII-dependent but antigen-independent mechanism, during which their antigen specificity is scanned for selective activation of cognate clones. Rapid migration and localization to high endothelial venules (HEVs) allow CD301b$^+$DCs to interact with incoming naive CD4 T cells immediately after their LN entry, which is impaired if the localization of CD301b$^+$DCs is disrupted by FTY720. These results indicate that migratory CD301b$^+$ DCs optimize the priming efficacy of CD4 T cells by serving as an immunological display window.

Results

Depletion of CD301b$^+$ DCs results in reduced accumulation of T and B Cells in the dLN

DCs are required for the immunization-induced LN hypertrophy, but subset-specific role of DCs in this process is poorly understood (4–6, 16). We previously showed that the size of the dLN early after immunization in CD301b$^+$DC-depleted mice was smaller than that in wild-type (WT) mice due largely to the impaired accumulation of CD4 T cells (14, 17). To address if CD301b$^+$ DCs directly regulate the recruitment and/or retention of lymphocytes, we transferred CFSE-labeled WT splenocytes retro-orbitally into diphtheria

toxin (DT)-treated WT (CD301b$^+$ DC-intact) or Mgl2-DTR (CD301b$^+$ DC-depleted) mice following subcutaneous immunization with ovalbumin (OVA) and papain in the right footpad (Fig. 1A). Two h after transfer, no differences were observed between WT and Mgl2-DTR recipients in the number of total donor splenocytes or their cellular composition in both right (draining) and left (non-draining) popliteal LN (Fig. 1B), indicating that the depletion of CD301b$^+$ DCs has no major impact on the lymphocyte entry into the LNs. Between 2 and 72 h transfer, the number of the donor CD4 T and CD8 T cells in the dLN increased two- to three-fold in the WT recipients, whereas the number of B cells increased by 36-fold (Fig. 1B), suggesting that many T cells that had homed to the dLN left the dLN relatively quickly, but most of the donor B cells remained in the dLN throughout this period. In the Mgl2-DTR recipients, the numbers of CD4 T cells, CD8 T cells and B cells were dramatically smaller than those in the WT recipients, with the most prominent reduction observed for CD4 T cells (Fig. 1B). Likewise, the numbers of host T and B cells in the dLN 96 h after immunization (72 h post-transfer) were smaller in the Mgl2-DTR hosts than those in the WT recipients (Fig. 1C). This was not due to differences in proliferation, as most of the donor cells were not dividing regardless of the CD301b$^+$ DC depletion status (Fig. S1A), which suggested that the reduction of donor cells was primarily due to changes in their trafficking. DT treatment of Mgl2-DTR mice resulted in an additional loss of epidermal Langerhans cells (which do not express CD301b) due to an unknown mechanism (14), but the reduction of donor cell accumulation was specifically caused by the depletion of CD301b$^+$ DCs, as the donor cell numbers were not affected in CD207-DTR mice, in which CD207$^+$ DC subsets, including Langerhans cells and dermal CD103$^+$ DCs, were depleted (Fig. 1D) (18–21).

CD301b$^+$ DCs are required for the upregulation of CD69 in polyclonal CD4 T cells recruited to the dLN

We previously showed that immunization of mice with a Th2-type adjuvant such as papain or alum results in upregulation of CD69 in endogenous CD4 T cells in a CD301b$^+$ DC-dependent manner (14). Consistent with this observation, CD69 was upregulated in both donor and host CD4 T cells in the dLN of WT recipients immunized with OVA and papain, but was dramatically attenuated in CD301b$^+$ DC-depleted recipients (Fig. 1E and 1F). Notably, among the donor T and B cells, CD69 upregulation was specific to CD4 T cells and was not affected by the depletion of CD207$^+$ DCs (Fig. 1E and 1G), suggesting that CD301b$^+$DCs were specifically required for the activation of CD4 T cells. CD69 can be induced in T cells by antigen-independent mechanisms such as type I interferons (IFN) (22), but here we observed that CD69 was upregulated in donor cells isolated from IFNα receptor (IFNAR)-deficient mice (Fig. 1H), suggesting that the CD69 upregulation in the donor CD4 T cells in this model was driven by TCR stimuli or inflammatory cytokines other than type I IFNs.

CD301b$^+$ DCs retain and activate naive polyclonal CD4 T cells in the dLN in an MHCII-dependent manner

The above data suggest that CD301b$^+$ DCs facilitate the retention of CD4 T cells in the dLN. Next, we transferred CFSE-labeled WT CD4 T cells into CD301b$^+$ DC-intact or depleted mice 24 h after footpad immunization with OVA and papain and then blocked

further LN entry with anti-CD62L blocking monoclonal antibody (mAb) 2 h after donor cell transfer (Fig. 2A) (23). This experimental setup allowed us to measure the LN dwell time for the donor CD4 T cells that had entered the LNs during the initial 2 h window. Donor cell entry to the LNs was blocked nearly completely after mAb injection, whereas the homing to the spleen, which does not require CD62L (24), remained intact (fig. S1B and S1C). In WT recipients, the donor CD4 T cells stayed in the dLN for at least 8 h and began to leave the dLN between 8 and 16 h after the CD62L blockade (Fig. 2B left panel, p=0.45 between 0 and 8 h, p=0.0011 between 0 and 16 h). The number of recruited CD4 T cell was dramatically lower, but the kinetics of the donor CD4 T cells in the contralateral non-draining (nd) LN followed a similar pattern, with the majority of donor CD4 T cells remaining in the LN for at least 8 h before leaving (Fig. 2B right panel, p=0.6183 between 0 and 8 h, p=0.0012 between 0 and 16 h). In contrast, the donor CD4 T cells in the CD301b$^+$ DC-depleted hosts failed to stay in the dLN and continuously decreased over time, whereas their retention in the ndLN was not impaired by depletion (Fig. 2B). The donor CD4 T cells that stayed in the dLN of WT recipients continuously upregulated CD69 during this time, which was markedly attenuated in CD301b$^+$ DC-depleted hosts (Fig. 2C and 2D). Collectively, these results indicate that CD301b$^+$ DCs are required for transient retention and activation of naive polyclonal CD4 T cells in the dLN.

Given the rarity of antigen-specific clones, it seemed unlikely that all CD69$^+$ donor CD4 T cells (>10% of the donor CD4 T cells in the dLN) were OVA- or papain-specific, but the IFNAR-independent upregulation of CD69 (Fig. 1H) nonetheless suggested the involvement of TCR-dependent activation. Indeed, CD69 upregulation by the donor CD4 T cells in the dLN was completely abrogated when transferred into MHCII-deficient hosts (Fig. 2E), further supporting the idea that the interaction between the host MHCII and the TCR on the polyclonal donor CD4 T cells is required for the CD69 upregulation.

Unlike CD8 T cells, the intranodal trafficking and LN dwell time of naive CD4 T cells are partially governed by the antigen presenting machinery (25, 26). In addition, the MHCII-dependent CD69 upregulation in CD4 T cells has been shown to correlate with their LN dwell time in naive LNs (27). To directly examine whether MHCII on CD301b$^+$ DCs plays a role in retaining polyclonal CD4 T cells, we generated mice expressing Cre recombinase in CD301b$^+$ cells (*Mgl2*$^{+/Cre}$ mice, fig. S2A) and crossed them onto mice with the I-Ab alleles flanked by two loxP cassettes (*H2ab1*$^{flox/flox}$). We noted partial reduction of CD301b protein expression in mice carrying the *Mgl2*^{Cre} allele as evidenced by the reduced CD301b$^+$ DC and compensatory increase in other cDC2 subsets in the *Mgl2*$^{Cre/Cre}$ mice (fig. S2B–S2D), but we nevertheless observed subset-specific loss of MHCII expression in CD301b$^+$ DCs in the resulting offspring (CD301b$^{\Delta MHCII}$ mice) (fig. S2E and S2F). Similar to CD301b$^+$ DC-depleted recipients, the donor polyclonal CD4 T cells in CD301b$^{\Delta MHCII}$ mice were retained in the dLN less efficiently than those in MHCII-intact hosts (Fig. 2F), and the upregulation of CD69 in the donor CD4 T cells was also impaired (Fig. 2G and 2H), indicating that MHCII expression in CD301b$^+$ DCs plays a role in transiently retaining and activating polyclonal CD4 T cells in the dLN. A similar phenotype was observed when total splenocytes were transferred into CD301b$^{\Delta MHCII}$ mice without CD62L blockade (fig. S2G). Notably, the reduction of CD69 upregulation in CD301b$^{\Delta MHCII}$ recipients was not as complete as in MHCII-deficient hosts (Fig. 2E), suggesting that the remaining MHCII$^+$ cells

and/or the residual MHCII expression in CD301b$^+$DCs (fig. S2F) may play a role in CD69 upregulation by CD4 T cells in those mice.

Our data suggest that CD301b$^+$DCs provide TCR stimulation for CD4 T cells upon their homing to the dLN. To further confirm that CD301b$^+$DCs directly stimulate the TCR of polyclonal CD4 T cells, we measured the expression levels of Nur77, a nuclear receptor whose expression levels directly correlate with the TCR signal strength (28–30), by transferring CD4 T cells isolated from the Nur77-GFP reporter mice (29). In WT recipients, the GFP expression was higher in the dLN than in the ndLN. In contrast, the GFP expression was similar between the dLN and ndLN in the CD301b$^{\Delta MHCII}$ mice as well as in MHCII-null recipients, indicating that CD301b$^+$DCs are a major source of the TCR stimulation (Fig. 2I). Collectively, these results indicate that CD301b$^+$ DCs transiently retain and activate polyclonal CD4 T cells in the dLN through MHCII-dependent interactions.

CD301b$^+$ DCs are necessary and sufficient for the naive CD4 T cell retention in the dLNs

CD301b$^+$ DCs account for a major fraction of skin-derived migratory DCs in the skin-dLNs (13, 14), thus it is possible that the impaired CD4 T cell retention in the CD301b$^+$ DC-depleted mice was due to the loss of a large number of DCs in general rather than to the specific loss of CD301b$^+$ DCs. To delineate the subset-specific role of CD301b$^+$ DCs in CD4 T cell retention, we generated a DC depletion mouse model in which CD301b$^+$ DCs are protected from the depletion. We targeted a DTR cassette flanked by two loxP sequences into the first intron of the *Itgax* allele (coding CD11c, fig. S2H) with a splice acceptor as previously described for an “inducible” CD11c-DTR mouse model (31). These mice (denoted CD11c-dlDTR hereafter) express a “deletable” DTR cassette in CD11c$^+$ cells, which can be removed from CD301b$^+$ cells when the CD11c-dlDTR mice were crossed with the Mgl2-Cre mice. DT treatment of the CD11c-dlDTR mice resulted in a reduction of the total DC population (fig. S2I) but left more CD301b$^+$ DCs intact than in the Mgl2-DTR mice, likely due to relatively low expression levels of the dlDTR cassette in CD301b$^+$ DC in this model (fig. S2J). This trend was further exaggerated in the Mgl2-Cre;CD11c-dlDTR mice, indicating successful removal of the dlDTR cassette from CD301b$^+$ cells in these mice (fig. S2J). Although this “protection” of CD301b$^+$ DCs from the DT-induced depletion in the Mgl2-Cre;CD11c-dlDTR mice did not result in increased relative abundance of CD301b$^+$ DCs in the total DC population compared to that in the CD11c-dlDTR mice (fig.S2K), we suspect that the number of CD301b$^+$ DCs in these mice are underestimated due to the reduction of CD301b protein expression in mice carrying the *Mgl2*^{Cre} allele (fig. S2B). Consistently, the relative abundance of CD172a$^+$ cDC2, a larger population of DCs that contains the CD301b$^+$ DCs in WT mice, was greater in the Mgl2-Cre;CD11c-dlDTR mice compared to the CD11c-dlDTR mice (fig S2L). Overall, the CD11c-dlDTR mice and Mgl2-Cre;CD11c-dlDTR mice had different degrees of depletion of the total DC population, but the relative abundance of CD301b$^+$ DCs within the total DC population in those mice remained similar to undepleted control animals (Fig. S2I and S2K). Importantly, the defect in CD4 T cell retention and CD69 upregulation was observed only in the Mgl2-DTR mice but not in either CD11c-dlDTR or Mgl2-Cre;CD11c-dlDTR mice, indicating that CD301b$^+$ DCs are both necessary and sufficient for the transient retention of CD4 T cells in the dLN (Fig. 2J and 2K).

CD301b$^+$ DC-dependent naive CD4 T cell retention in the dLN is irrespective of TCR specificity

The above data indicates that the interaction between the TCR on CD4 T cells and MHCII in CD301b$^+$DCs is necessary, but it remains unclear if the cognate interaction involving a specific foreign peptide is required for the CD301b$^+$ DC-dependent retention of CD4 T cells in the dLN. To clarify the role of cognate and non-cognate interactions in CD301b$^+$DC-dependent CD4 T cell trafficking, we co-transferred OVA-specific *Rag1*$^{-/-}$ OT-II TCR transgenic CD4 T cells and WT naive polyclonal CD4 T cells into CD301b$^+$ DC-intact or CD301b$^+$ DC-depleted mice that had been immunized with OVA and papain and assessed their LN dwell time (Fig. 3A). To our surprise, the trafficking kinetics of the antigen-specific CD4 T (OT-II) cells was similar to polyclonal counterparts in spite of the presence of cognate antigen (Fig. 3B). In the WT recipients, the numbers of both OT-II and WT CD4 T cells in the dLN remained similar for at least 8 h before starting to decrease. In contrast, in the CD301b$^+$ DC-depleted recipients, the numbers of both donor cell types continued to decrease, suggesting that CD301b$^+$DCs are required for the CD4 T cell retention regardless of the presence of cognate antigen.

The above results suggest antigen-independence of the CD301b$^+$ DC-dependent CD4 T cell retention, but it is possible that antigen (papain)-specific clones among the donor polyclonal CD4 T cells were selectively retained in the dLN. To formally exclude this possibility, we repeated the same experiment as in Fig. 3A, except that the recipients were immunized with papain alone without OVA so that there was no cognate antigen for the *Rag1*$^{-/-}$ OT-II cells. Similar to the results described above, the numbers of both *Rag1*$^{-/-}$ OT-II and polyclonal CD4 T cells retained in the dLN were dramatically lower in the CD301b$^+$ DC-depleted hosts (Fig. 3C). Taken together, these results indicate that CD301b$^+$ DCs transiently retain naive CD4 T cells regardless of their TCR specificity.

CD301b$^+$ DC-dependent CD69 upregulation is antigen-dependent

Under inflammatory conditions, CD69 is induced in T cells in a manner dependent on T cell-intrinsic IFNAR and inhibits their egress from the dLN by downregulating sphingosine 1-phosphate (S1P) receptor S1PR1 (22). Our previous studies indicate that CD301b$^+$DC depletion also results in a reduction in CD4 T cell accumulation in the dLN in mice immunized with OVA and CpG without causing a reduction in CD69 expression (14). To examine if CD301b$^+$ DCs are required for the retention of polyclonal CD4 T cells under non-Th2 immunization conditions, we immunized mice in the footpad with OVA emulsified in complete Freund's adjuvant (CFA) (fig. S3A). As in mice immunized with papain, the donor CD4 T cells in CD301b$^+$ DC-depleted mice spent a shorter time in the dLNs than those in WT mice (fig. S3B). Their CD69 expression levels were comparable, which suggested that differences in CD69 expression alone did not account for the shorter dwell time in CD301b$^+$ DC-depleted mice (fig. S3C). Similar results were obtained in CD301b$^{\Delta MHCII}$ mice (fig.S3D and S3E).

CD69 is generally thought to promote transient retention of activated T cells in the dLN (22), so we further examined the role of antigen recognition in papain-induced CD69 upregulation by co-transferring *Rag1*$^{-/-}$ OT-II and WT polyclonal CD4 T cells and

comparing their CD69 expression levels in mice immunized with either OVA plus papain or papain alone. In mice immunized with OVA plus papain, more than 50% of the OT-II cells in the dLN had upregulated CD69 at the time of CD62L blockade (2 h after the OT-II cell transfer) in WT hosts, whereas only about 25% had done so in CD301b$^+$DC-depleted hosts (Fig. 3D). Eight h after the CD62L blockade, the majority of OT-II cells in the dLN expressed CD69 in both WT and CD301b$^+$ DC-depleted recipients, but expression levels were slightly but significantly reduced in the latter ($p = 0.0031$ between WT and CD301b$^+$ DC-depleted mice) (Fig. 3D, see also Fig. 6H). Given that many OT-II cells fail to stay in the dLN of CD301b$^+$ DC-depleted recipients during this time, the data suggest that CD69 upregulation 8 h after the dLN entry was too late and/or not sufficient to prevent CD4 T cells from leaving the dLN of those mice. As shown in Fig. 2, CD69 upregulation was also observed in the donor polyclonal CD4 T cells in the dLN of WT recipients but was impaired in the CD301b$^+$ DC-depleted recipients (Fig. 3D). Similarly, CD69 upregulation in donor polyclonal CD4 T cells was CD301b$^+$DC-dependent in mice immunized with papain alone (Fig. 3E and 3F). Even though there was a clear, antigen-nonspecific upregulation of CD69 induced by papain alone in the donor *Rag1*$^{-/-}$ OT-II cells in the dLN compared to those in the ndLN, it was not impaired by the depletion of CD301b$^+$ DCs (Fig. 3E and 3F). Antigen-dependent and independent CD69 upregulation was also observed in *Rag1*$^{+/-}$ OT-II cells when *Rag1*$^{-/-}$OT-II, *Rag1*$^{+/-}$ OT-II and polyclonal CD4 T cells were co-transferred (fig. S4).

IFNAR in CD4 T cells is not required for CD69 expression 3 days after adoptive transfer (Fig. 1H), but its requirement for the retention and CD69 expression by CD4 T cells early after their dLN entry remains unclear. To further clarify the role of IFNAR signaling in CD4 T cell retention, we co-transferred WT and *Ifnar*$^{-/-}$ polyclonal CD4 T cells into CD301b$^+$ DC-intact and depleted recipients that had been immunized with OVA plus papain and measured their dLN dwell time and CD69 expression after CD62L blockade. WT and *Ifnar*$^{-/-}$ CD4 T cells showed no difference in their dLN dwell time, with both showing significantly shorter dwell time when CD301b$^+$ DCs were depleted (Fig. 3G). Likewise, CD69 upregulation was similar between WT and *Ifnar*$^{-/-}$ CD4 T cells and was similarly impaired in the CD301b$^+$ DC-depleted hosts (Fig. 3H), again confirming the indispensable role for CD301b$^+$ DCs in CD69 upregulation but not for IFNAR signaling. There was a small, transient reduction in CD69 expression in *Ifnar*$^{-/-}$ CD4 T cells compared with their WT counterparts in CD301b$^+$ DC-depleted recipients 8 h after the dLN entry (Fig. 3H). These data indicate that, while the IFNAR signaling is partially required for the CD301b$^+$DC-independent CD69 upregulation in CD4 T cells, it is not required for their retention in the dLN.

Taken together, these results indicate that, upon immunization with papain, CD69 is upregulated in CD4 T cells in both antigen-dependent and independent manner. While the requirement of CD301b$^+$ DCs for the CD4 T cell retention in the dLN is independent of the TCR specificity (Fig. 3C), CD301b$^+$ DCs are required only for the antigen-dependent CD69 upregulation in CD4 T cells (Fig. 3D–3F). Although these experiments do not address whether CD69 is *required*, the data suggest that its upregulation alone is *not sufficient* for inducing the retention of CD4 T cells in CD301b$^+$ DC-depleted mice. Since *Rag1*$^{-/-}$ and

Rag1$^{+/-}$ OT-II cells behaved similarly, we used *Rag1*$^{+/-}$ OT-II cells to examine the role of CD301b$^+$ DCs in antigen-specific CD4 T cell responses in the following experiments.

CD301b$^+$ DCs directly present soluble foreign antigens to CD4 T cells in the dLN immediately after their homing

The above data suggest that CD301b$^+$DCs provide CD4 T cells with (1) MHCII-dependent but antigen-independent signal to transiently stay in the dLN and (2) MHCII- and antigen-dependent signal to upregulate CD69 expression. This latter signal likely represents the direct antigen presentation to the cognate CD4 T cell clones. Previous studies show that CD301b$^+$ DCs are enriched at the T-B cell border area in the LN and segregated from CD207$^+$ DCs (including epidermal Langerhans cells and dermal CD103$^+$ DCs), which preferentially localize to the deeper T cell zone (13, 18, 32). In WT mice immunized with OVA and papain, CD301b$^+$ DCs were also enriched at the T-B boundary areas and located in closer proximity the HEVs than CD207$^+$ DCs (Fig. 4A–4C). The depletion of CD301b$^+$ DCs did not affect the relative positioning of CD207$^+$ DCs to the HEVs, suggesting that their distance to HEVs is determined by their intrinsic mechanism (Fig. 4C).

We previously showed that CD301b$^+$ DCs represent the majority of hapten-bearing skin-derived migratory cells that appear in the dLN 24 h after epicutaneous painting with a fluorescent hapten such as FITC or TRITC with a skin irritant di-*n*-butyl phthalate (DBP) (13, 14). When WT mice were subcutaneously immunized with OVA and papain and simultaneously painted with TRITC (without DBP) on the skin at the immunization site, > 60% of TRITC$^+$ MHCII$^+$ cells expressed CD301b in the dLN 24 h after immunization, and ~30-40% of the total CD301b$^+$ cells in the dLN was TRITC$^+$ (fig. S5A–S5F). In addition, the depletion of CD301b$^+$ cells resulted in a dramatic reduction of the total TRITC$^+$ cells in the dLN (fig. S5A and S5D). TRITC is carried to the dLN by migratory DCs rather than by passive diffusion (33), so these data indicate that CD301b$^+$ DCs are a major migratory DC subset mobilized by papain. Likewise, when mice were immunized with fluorescently labeled OVA and papain, CD301b$^+$ DCs had a higher percentage of OVA-loaded cells compared with other DC subsets in the dLN (Fig. 4D, S5G and S5H), indicating that CD301b$^+$ DC efficiently take up and transport the OVA protein to the dLN. Although OVA$^+$ B cells outnumbered any OVA$^+$ DC subset due to the abundance of the total B cells, the amount of OVA per cell in B cells was minimal, suggesting that B cells are not the major antigen-presenting cells (Fig. 4E and S5H). Notably, when the mice were immunized with OVA and CFA, both CD301b$^+$ DCs and CD103$^+$ DCs took up the antigen at similar levels (fig. S5I and S5J). However, in either case, the depletion of CD301b$^+$ DCs had a minimal impact on the amount of OVA transported to the dLN by other antigen presenting cells (Fig. 4D and fig. S5I).

We next examined whether CD301b$^+$ DCs directly interact with the antigen-specific CD4 T cells in the dLN by attempting to detect cellular conjugates between CD4 T cells and CD301b$^+$ DCs formed in the dLN by flow cytometry. We transferred Nur77-GFP;CD45.1;OT-II cells into WT (CD45.1$^-$) recipients immunized with OVA and papain one day earlier and analyzed dLNs 3 and 24 h after the transfer without excluding doublets (Fig. 4F). A small population of CD45.1$^+$ MHCII$^+$ doublets was detected, indicating stable

interactions between the CD45.1$^+$ OT-II cells and the host MHCII$^+$ cells (Fig. 4G and S6A). The majority of these doublets were formed *in vivo* in the dLN and not *ex vivo* in cell suspensions, as no fluorochrome exchange was observed when two sets of LN cells were separately stained for CD45.1 and MHCII with different sets of fluorochromes and mixed together *in vitro* as previously described (fig. S6B) (34, 35). The CD45.1$^+$ MHCII$^+$ doublets were reduced when the mice were immunized with papain alone, indicating the antigen dependency of this interaction (fig. S6C–S6G). B220$^+$ CD11c$^-$ B cells contributed to a large portion of the doublets, and this interaction seemed to be antigen-independent because similar interactions was detectable after immunization with papain alone, whereas CD301b$^+$ DC-OT-II cell interactions were largely dependent on the presence of OVA (fig. S6D and S6E). Three hours after the OT-II cell transfer, ~25% of the CD45.1$^+$MHCII$^+$ doublets contained CD301b$^+$ DCs (Fig. 4H). When compared with the DC subset composition in the host-derived singlet MHCII$^+$ cells, CD301b$^+$ DCs were significantly more enriched in the OT-II doublets over CD207$^+$ and double negative (CD301b$^-$ CD207$^-$) DCs or B cells (Fig. 4I). The enrichment of CD301b$^+$ DCs in the CD45.1$^+$ MHCII$^+$ doublets was similar between 3 and 24 h after the OT-II cell transfer, but greater enrichment of CD301b$^-$ CD207$^-$ DCs was detected at the latter time-point, suggesting that the donor OT-II cells primarily interact with CD301b$^+$ DCs early after their homing to the dLN, but later interact with other DC subsets (Fig. 4H and 4I). In contrast, in recipients immunized with OVA and CFA, all DC subsets (CD301b$^+$, CD207$^+$ and CD301b$^-$ CD207$^-$ DCs) showed similar enrichment in either time-point, suggesting the additional involvement of CD301b$^-$ DCs in early CD4 T cell priming under type 1 immunization conditions (fig. S6H–S6J). The majority of OT-II cells expressed the Nur77-GFP reporter and CD69 3 h after transfer upon conjugation with any DC subset, whereas only about a half of the OT-II cells conjugated with B cells expressed these markers (Fig. 4J–4L and fig. S6K–S6M), indicating that DCs but not B cells are the primary antigen presenting cells. These results suggest that CD301b$^+$ DCs directly present soluble foreign antigens to cognate CD4 T cells immediately after their dLN entry.

The positioning of CD301b$^+$ DCs near HEVs facilitates their interaction with incoming naive CD4 T cells

HEV-derived S1P has been shown to indirectly recruit skin-derived DCs to areas near HEVs by inducing production of CCR7 ligands by high endothelial cells themselves, and the blockade of S1P signaling with an S1P receptor functional antagonist FTY720 sequesters DCs from those areas (36). To examine if this mechanism accounts for the localization of CD301b$^+$ DCs near the HEVs, we treated WT mice with FTY720 and concurrently immunized with OVA and papain. FTY720 treatment did not alter the frequencies or total numbers of migratory DC subsets in the dLN (Fig. 5A) but was associated with CD301b$^+$ DCs moving away from HEVs without affecting the positioning of CD207$^+$ DCs relative to the HEVs or to CD301b$^+$ DCs (Fig. 5B–D). To further elucidate the functional importance of the positioning of CD301b$^+$ DCs, we transferred OT-II or WT CD4 T cells into WT recipients that had been treated with FTY720 or vehicle and immunized with OVA and papain one day prior, and then blocked LN entry using CD62L mAb 1.5 h after transfer (Fig. 5E). At the time of the LN entry block, the number of OT-II cells in the dLN was comparable between the vehicle- and FTY720-treated groups (Fig. 5F), indicating that FTY720 has little or no impact on the CD4 T cell entry to the dLNs. Notably, CD69

expression in the donor OT-II cells was significantly reduced in the FTY720-treated mice at this time-point (Fig. 5G). Unlike CD301b$^+$ DC-depleted mice, the FTY720-treated mice showed no reduction in the dLN dwell time of donor OT-II cells due to the inhibitory effect of FTY720 on lymphocyte egress (Fig. 5F), but nonetheless showed impaired DC-T cell conjugate formation early after the entry of OT-II cells in to the dLN (Fig. 5H), although the conjugates in FTY720-treated mice were too rare to analyze their DC subset composition. The reduction of CD69 expression was not likely due to direct inhibition of T cell activation by FTY720, as the CD69 expression in the donor OT-II cells became nearly comparable between the two groups by 8 h after their LN entry (Fig. 5G) whereas FTY720 still remained effective as indicated by the lack of donor cell egress (Fig. 5F). Similar results were obtained when WT polyclonal CD4 T cells were adoptively transferred into FTY720-treated recipients (Fig. 5I and 5J). These results largely recapitulate the delay in CD69 upregulation in the donor CD4 T cells in CD301b$^+$ DC-depleted mice (Fig. 3D and 3E) and thus indicate that the strategic positioning of CD301b$^+$ DCs near the HEVs ensures their early access to incoming naive CD4 T cells.

CD301b$^+$DCs are required for timely priming of antigen-specific CD4 T cells

To examine the role of CD301b$^+$ DCs in antigen-specific CD4 T cell priming and the subsequent expansion, we monitored the activation kinetics of CFSE-labeled OT-II cells in WT or CD301b$^+$ DC-depleted recipients. The priming was semi-synchronized by blocking CD62L two h after transferring OT-II cells into mice immunized with OVA and papain one day prior (Fig. 6A). In both CD301b$^+$ DC-intact and depleted mice, most OT-II cells remained undivided for up to 16 h post-CD62L blockade (Fig. 6B). More than a half of the OT-II cells underwent the first cell division between 16 and 32 h post-CD62L blockade in WT mice (Fig. 6B and 6C). In CD301b$^+$ DC-depleted mice, however, only about 20% of the OT-II cells had divided during this period, suggesting a delay in their initial cell cycle entry (Fig. 6B and 6C). This was also reflected in the significantly fewer cell division cycles at 56 h post CD62L blockade (Fig. 6B and 6C). As was observed in mice co-transferred with OT-II and WT CD4 T cells (Fig. 3), the number of OT-II cells remained in the dLN 8 h after CD62L blockade was dramatically lower in the CD301b$^+$DC-depleted mice than in WT mice, but the difference between the two groups disappeared as the majority of the OT-II cells left the dLN by 16 h after homing blockade (Fig. 6D inset). However, only a minimal expansion of OT-II cells in CD301b$^+$DC-depleted mice was detected by 56 h, likely due to the delayed cell division, whereas the number of OT-II cells was dramatically increased in WT mice between 32 and 56 h post-CD62L blockade (Fig. 6D). This also resulted in a striking reduction in the percentage of OT-II cells within the total CD4 T cell population in CD301b$^+$DC-depleted mice (Fig. 6E), which was partially accounted for by increased cell death in OT-II cells (Fig. 6F). These results collectively indicate that CD301b$^+$DCs are required for the timely priming and maximal expansion of antigen-specific CD4 T cells during the early priming phase.

We analyzed the expression of early activation markers in OT-II cells during the early priming phase, and 8 h after CD62L blockade, > 90% of the OT-II cells in WT recipients had already upregulated CD69, and a part of the CD69$^+$ OT-II cells at this time-point co-expressed Nur77 (Fig. 6G–6I). The expression of CD69 and Nur77 gradually decreased

over time and returned to basal levels by 56 h post-CD62L blockade. As in Fig. 3D, CD69 expression in the donor OT-II cells in CD301b$^+$DC-depleted mice was reduced at earlier time-points but later recovered, suggesting a delay but not total loss of TCR stimulation (Fig. 6G and 6H). In contrast, the Nur77 expression in the donor OT-II cells remained lower in the CD301b$^+$ DC-depleted recipients than in WT recipients throughout the time-points analyzed, suggesting attenuation in TCR signal strength (Fig. 6I). Similarly, priming of OT-II cells in the CD301b$^{\Delta MHCII}$ mice also resulted in a delay in cell cycle entry and CD69 upregulation as well as in impaired Nur77 expression (fig. S7). The use of Nur77-GFP;OT-II cells did not further clarify these differences due to its high sensitivity and relatively binary reporter activity in monoclonal TCR transgenic T cells (37), as most of the OT-II cells expressed GFP at the brightest levels regardless of the CD301b$^+$ DC depletion, which further supports our interpretation that TCR stimulation is still present in the CD301b$^+$ DC-depleted recipients (Fig. 6J). Taken together, these results indicate that CD301b$^+$DCs are required for the timely and maximal stimulation of antigen-specific CD4 T cell clones, but other antigen presenting cells can eventually provide TCR stimulation even if CD301b$^+$DCs are depleted.

Early interaction with CD301b$^+$DCs is critical for the maximal expansion and the fate decision by antigen-specific CD4 T cells

The data thus far indicated a crucial role for CD301b$^+$ DCs in the initial activation and cell cycle entry of antigen-specific CD4 T cells, so we hypothesized that there is a critical time window in which CD301b$^+$ DCs are required. To test this possibility, we depleted CD301b$^+$ DCs at two different time points (before or after the initial cell division) and examined their impact on the OT-II cell division (Fig. 7A). Similar to the above experiments in which CD301b$^+$DCs were depleted one day before the immunization (Fig. 6A), the depletion of CD301b$^+$ DCs one day after the immunization resulted in fewer cell divisions when analyzed 56 h after their dLN entry (Fig. 7B). In contrast, there was no impact on OT-II cell division when CD301b$^+$ DCs were depleted two days after immunization (Fig. 7B), indicating that CD301b$^+$ DCs are required for the timely cell cycle entry of antigen-specific CD4 T cells rather than their continued proliferation.

To examine whether the requirement of CD301b$^+$ DCs for the optimal expansion of antigen-specific CD4 T cells is specific to Th2 conditions, we immunized the mice with OVA and CFA. Similar to mice immunized with OVA and papain, OT-II cells in the CD301b$^+$ DC-depleted mice showed a small but significant reduction in the number of cell divisions ($p = 0.021$ between WT and CD301b$^+$ DC-depleted mice) (Fig. 7C and 7D), which also led to a reduction in the number of OT-II cells in the dLN (Fig. 7E). These results indicate that CD301b$^+$ DCs are required for the optimal priming and maximal expansion of antigen-specific CD4 T cells under both Th2 and non-Th2 immunization conditions.

We previously reported that depletion of CD301b$^+$ DCs abolishes Th2 cell differentiation of antigen-specific CD4 T cells, whereas their differentiation into Th1 cells remains largely unaffected (14). The requirement of CD301b$^+$ DCs for Th2 differentiation is specific to this DC subset, as the depletion of CD207$^+$ DCs (including epidermal Langerhans cells and dermal CD103$^+$ DCs) did not affect Th2 differentiation (fig. S8). Since the critical

time-window for the interaction between CD301b$^+$ DCs and antigen-specific CD4 T cells is narrow (Fig. 7B), it is possible that the lagged priming of recirculating OT-II cells had masked the impact of CD301b$^+$ DC depletion on Th1 differentiation in our previous experiments, as those experiments did not employ the semi-synchronized priming model. To examine the direct impact of the CD301b$^+$ DC depletion on the fate decision by antigen-specific CD4 T cell clones primed in a semi-synchronized setting, we transferred OT-II cells and immunized mice as in Fig. 6A and restimulated the dLN cells *ex vivo* 80 h after CD62L blockade. The reduction in IL-4$^+$ Th2 cells did not reach statistical significance at this time point, but their differentiation into IFNγ^+ Th1 cells was significantly enhanced in CD301b$^+$ DC-depleted mice (Fig. 7F). In addition, the expression of IL-4 receptor α in OT-II cells was reduced in CD301b$^+$ DC-depleted mice 56 h after CD62L blockade, suggesting that the OT-II cells had already been skewed against Th2 differentiation in the CD301b$^+$ DC-depleted mice by that time (Fig. 7G). Consistent with this observation, IL-4 reporter expression was reduced in CD301b$^+$ DC-depleted hosts at this time point when OT-II mice of *Il4-GFP* (4get) background were used as the donor (Fig. 7H). In addition, mice immunized with OVA and CFA showed enhanced expression of IFNγ and IL-17A in OT-II cells with depletion of CD301b$^+$ DCs (Fig. 7I). These results suggest that early interactions with CD301b$^+$ DCs during the priming of antigen-specific CD4 T cells generally promotes Th2 differentiation while suppressing their differentiation into Th1 and Th17 cells.

CD301b$^+$ DCs are required for optimal priming and expansion of rare antigen-specific CD4 T cell clones

Under physiological conditions, DCs scan millions of naive CD4 T cells to find antigen-specific clones. Based on the above data, we hypothesized that the primary role of CD301b$^+$ DCs is to scan incoming polyclonal CD4 T cells upon dLN entry and find rare antigen-specific clones. To test this hypothesis, we transferred titrated numbers of OVA-specific OT-II cells (1, 10, 100, 1000, or 10,000 cells) into CD301b$^+$ DC-intact or depleted mice that were immunized with OVA and papain for 24 h without CD62L blockade and enumerated OT-II cells in the dLN 4 days after transfer (Fig. 8A). The numbers of recovered OT-II cells were constantly smaller in CD301b$^+$ DC-depleted mice than in CD301b$^+$ DC-intact mice, which was more exaggerated when the input OT-II cell numbers were lower (100 or 1000 input cells compared with 10,000 input cells, Fig. 8B and 8C). Similarly, the numbers of recovered OT-II cells were constantly smaller in CD301b$^{\Delta MHCII}$ mice compared with the MHCII-intact recipients when a lower number of OT-II cells were transferred (Fig. 8D), indicating that CD301b$^+$ DCs maximize the priming efficiency of rare antigen-specific CD4 T cell clones through MHCII-dependent interactions. The potential discrepancy between the results described in Fig. 6D (that the CD301b$^+$ DC depletion results in impaired expansion of OT-II cells) and the results from the mice with higher input OT-II cell numbers (showing no significant reduction in the output OT-II cell numbers when 10,000 OT-II cells were transferred) is likely due to the lack of CD62L blockade in the latter, as lagged priming of the recirculating OT-II cells may mask their impaired priming efficacy especially when the number of recirculating OT-II cells is high.

To further confirm the role of CD301b$^+$ DCs in maximizing the priming efficacy of rare antigen-specific CD4 T cells, we transferred a high number ($1x10^5$) of OT-II cells into

WT or Mgl2-DTR recipients, immunized with OVA and papain in the right footpad, and re-challenged them in the left footpad 16 days later, when the primary response was fully contracted (Fig. 8E and fig. S9A–S9C). The secondary challenge induced a massive re-expansion of the OT-II cells in the left dLN of WT mice. In contrast, the re-expansion was minimal when CD301b$^+$ DCs were depleted immediately before the secondary immunization (Fig. 8F and 8G). Unlike the above experiments in which OT-II cells were transferred 1 day after immunization, these experiments show the requirement of CD301b$^+$ DCs for the priming of pre-existing OT-II cells, eliminating the possibility that the abovementioned role of CD301b$^+$ DCs is dependent on the timing of OT-II cell transfer.

Lastly, to address if CD301b$^+$ DCs are also required for the priming and expansion of endogenous antigen-specific CD4 T cells, we examined the expression of TCRVα2, the dominant Vα chain expressed by endogenous CD4 T cells that recognize an immunodominant OVA peptide presented by I-A^b MHCII molecule (38). The depletion of CD301b$^+$ DCs before the primary immunization or the secondary challenge resulted in a reduction in the number of TCRVα2$^+$ effector CD4 T cells in the dLN of each respective site (fig. S9D–S9F).

Collectively, these results indicate that CD301b$^+$ DCs are required for optimal priming and expansion of rare antigen-specific CD4 T cell clones.

Discussion

The kinetics of antigen-specific CD4 T cell priming is a critical determinant of immunological outcomes and is heavily affected by the frequency of antigen-specific naive CD4 T cells and the timing of priming (23, 39–41). While the molecular mechanism of CD4 T cell trafficking and activation has been extensively studied, the cellular mechanism that maintains the number of CD4 T cells in the reactive dLN for effective priming is less well understood. Here we show that CD301b$^+$ DCs (1) transiently retain naive polyclonal CD4 T cells through the MHCII-dependent interaction regardless of the TCR specificity, (2) directly present antigens to CD4 T cells upon their dLN entry to induce early activation of antigen-specific CD4 T cells, (3) promote Th2 differentiation while suppressing the Th1 and Th17 commitment, and (4) are required for the robust and timely expansion of rare antigen-specific CD4 T cell clones during the primary and recall responses.

DCs and CD4 T cells cooperatively accelerate the cellular influx to the dLN (5, 6, 16). Although it is generally assumed that immunization-induced dLN hypertrophy is associated with both increased cellular influx and decreased egress (22, 42–45), earlier studies demonstrated that the egress shutdown, if any, is transient and is followed by a larger-than-usual efflux from the dLN, making the number of lymphocytes passing through the LN per time unit much larger for the dLN than for the ndLN (46, 47). Nonetheless, despite the huge difference in total cellularity, our data show no major changes in the LN dwell time of naive CD4 T cells between the dLN and ndLN in WT hosts, suggesting the wide capacity range of LNs to scan incoming CD4 T cells at a relatively constant rate. In fact, the egress of polyclonal CD4 T cells in WT mice was non-linear, with no apparent egress within the first 8 h after their LN entry. Importantly, the CD301b$^+$ DC-depleted mice

lost the ability to hold CD4 T cells during this 8 h window in the dLN but not in the ndLN, suggesting that CD301b$^+$ DCs are mobilized to meet the increased demand for scanning polyclonal CD4 T cells and serve as an immunological “display window” that temporarily retains the incoming CD4 T cells in the dLN. To our surprise, the dLN transit time was similar between polyclonal CD4 T cells and antigen-specific OT-II cells and was similarly reduced in CD301b$^+$DC-deleted mice as well as in CD301b$^{\Delta MHCII}$ mice, indicating that the transient retention is dependent on MHCII but not on the antigen, and it is conceptually distinct from the well-characterized retention of T cells through cognate interaction (1–3). In accordance with our data, mathematical models predict that the intensive scanning of T cells by DCs (thus longer LN dwell time) maximizes the priming efficacy when the antigen density and the frequency of antigen-specific clones are low (48). Our data indicate that CD301b$^+$DCs are required for the antigen-dependent upregulation of CD69 in CD4 T cells, but also show that the CD69 upregulation alone was not sufficient for preventing them from leaving the dLN if CD301b$^+$ DCs are absent. Previous studies show that continuous interaction of naive CD4 T cells with DCs presenting the self peptide-MHCII complexes in naive LNs slows down the LN transit of CD4 T cells, induces partial expression of CD69 and helps naive CD4 T cells to maintain their sensitivity to cognate peptides (25–27, 49, 50). While such “sensitivity maintenance” of CD4 T cells through the self peptide-MHCII interaction may also be provided by CD301b$^+$ DCs, further study is needed regarding the signaling events triggered upon antigen-independent engagement with CD301b$^+$ DCs.

cDC2 subsets, including CD301b$^+$DCs, prime CD4 T cells more efficiently than the cDC1 cells and are often required for the differentiation of antigen-specific CD4 T cells into Th2 and/or Th17 effector cells (9, 12, 14, 51–59). However, in contrast to the general requirement of cDC1 cells for CD8 T cell priming (60, 61), there is no single cDC2 subset that is known to be absolutely required for CD4 T cell priming. Our data show that CD301b$^+$DCs play a unique role in efficient scanning of antigen specificity, timely priming and expansion, and Th2 differentiation of antigen-specific CD4 T cells. Notably, while CD301b$^+$DCs were also required for the maximal CD4 T cell retention and expansion under the type 1 immunization condition with CFA, they concurrently suppressed Th1 and Th17 differentiation. These reciprocal roles may operate as a safety threshold to avoid overt activation of Th1- and/or Th17-driven inflammation and suggest potential cooperation between CD301b$^+$DCs and CD301b$^-$DCs in Th1/Th17 priming as previously proposed for migratory and LN-resident DCs (62, 63).

Upon immunization in the skin, CD301b$^+$ dermal DCs migrate to the dLN earlier than other migratory DC subsets (13, 14, 18, 64, 65). This quick mobilization is facilitated by the direct sensing of the irritants by skin-innervating neurons (66–68), but its immunological advantage has not been fully addressed. Our data suggest that their rapid migration and localization to the HEVs ensures timely priming of CD4 T cells. CD4 T cells are primed by antigen-bearing migratory DCs at the outer edge of the T cell zone where the HEVs are enriched (69–71), or, alternatively, in the areas adjacent to the lymphatic sinuses by LN-resident cDC2 cells that sample antigens directly from the sinus (9, 10). While not mutually exclusive, the latter mode does not require DC migration and can induce a quick response, particularly when the antigen rapidly disperses through the lymphatics into the dLN that is preseeded by a sufficient number of antigen-specific CD4 T cells. In contrast,

the former migratory DC-dependent mechanism may be more important for antigens that are strictly restricted to the peripheral organs (9–11, 72). However, the full CD4 T cell response often requires migratory DCs even when the CD4 T cell priming by LN-resident DCs precedes the arrival of migratory DCs in the LN (10, 11). Importantly, our data suggest that, even under certain conditions in which LN-resident DCs play a predominant role in antigen-specific CD4 T cell priming (9, 10), CD301b$^+$ DCs are still required for maximizing the polyclonal CD4 T cell pool for effective priming. Consistent with our observation, a recent study shows that the EBI2-dependent localization of naive CD4 T cells to the outer T cell zone facilitates the priming of antigen-specific CD4 T clones especially when the antigen dispersal and cognate clones are limited (70).

Collectively, our results demonstrate that CD301b$^+$ DCs dictate the dynamics of the CD4 T cell response against soluble antigens in the LN. One of the main limitations of our study is the lack of quantitative assessment of their role with regards to the dose and clearance kinetics of the antigen. Continuous presence of antigen under certain conditions such as infection may facilitate CD4 T cell priming by widening the time window for repertoire scanning, rather than by increasing the scanning efficacy as proposed in our model. Further studies are needed to decipher their role in responses against particulate, cell-associated, or replicating antigens as well as the molecular mechanism of their subset-specific interaction with CD4 T cells.

Materials and Methods

Study design (please summarize study here)

The aim of this study was to understand the role of CD301b$^+$ cDC2 cells in CD4 T cell priming in the skin-dLN. To that end, we used multiple mouse models in which specific cDC subset(s) can be selectively depleted or genetically manipulated, and examined antigen-specific and polyclonal CD4 T cell responses to a model antigen OVA and model adjuvants papain and CFA by flow cytometry and immunohistochemistry. CD4 T cell priming were semi-synchronized by blocking CD62L in some adoptive cell transfer experiments in order to measure the LN transit time of CD4 T cells that homed to the dLN within a specific time-window.

Mice

Mgl2-DTR and *Mgl2*^{Cre} mice were a gift from Akiko Iwasaki (Yale University). Generation of *Mgl2*^{Cre} and CD11c-dlDTR mice is described in Supplementary Methods. C57BL/6 (B6) and congenic CD45.1 (B6.SJL-PtprcaPep3b/BoyJ) mice on B6 background were purchased from Charles River Laboratory and propagated in our colony. MHCII$^{fl/fl}$ (B6.129X1-H2-Ab1^{tmKoni}/J), MHCII$^{-/-}$ (B6.129S2-H2$^{dlAb1\text{-}Ea}$/J), OT-II (B6.Cg-Tg(TcraTcrb)425Cbn/J), CD207-DTR (B6.129S2-Cd207$^{tm3(DTR/GFP)Mal}$/J), *Rag1*$^{-/-}$ (B6.129S7-Rag1tm1Mom/J) and Nur77-GFP reporter (C57BL/6-Tg(Nr4a1-EGFP/cre)820Khog/J) mice were purchased from the Jackson Laboratory (Bar Harbor, ME) and maintained in house. *IFNAR*$^{-/-}$ mice and the OT-II mice on the IL-4-GFP background (4get;OT-II) were gift from Karen Edelblum and Jason Weinstein, respectively (Rutgers New Jersey Medical School). Mgl2-DTR mice (B6.*Mgl2*$^{+/DTR\text{-}EGFP}$) were previously described and maintained in our

colony (14). OT-II mice were crossed with CD45.1 mice to generate CD45.1;OT-II mice. The CD45.1;OT-II mice were maintained on the *Rag1*$^{-/-}$ background and used for some experiments. Nur77-GFP mice were crossed with CD45.1 or CD45.1;OT-II mice to generate CD45.1;Nur77-GFP or CD45.1;Nur77-GFP;OT-II mice, respectively. The 4get;OT-II mice were crossed with CD45.1 mice to generate CD45.1;4get;OT-II mice. All animal experiments in this study have been approved by the Institutional Animal Care and Use Committee at Rutgers New Jersey Medical School.

DT treatment and immunization

For DC depletion, mice were injected with 500 ng DT (List Biological Laboratories) intraperitoneally at indicated time-points. All immunization procedures were performed in the rear footpad with 20 μL injection volume per footpad as described previously (14). Mice were immunized as indicated in each Fig. with 5 μg low-endotoxin OVA (Worthington Biochemical Corporation) together with 50 μg papain (P4762, Sigma) or 10 μL CFA (F5881, Sigma). For *in vivo* antigen-uptake experiments, OVA was labeled with Alexa Fluor 488 Protein Labeling Kit (A10235, Thermo Fisher) and injected (5 μg) in the rear foot pad together with 50 μg papain or with 10 μL CFA. The ipsilateral (dLN) and contralateral (ndLN) popliteal LNs were harvested at indicated time-points.

Cell trafficking and priming analysis

For all cell transfer experiments, the donor cells were isolated from naive mice and the indicated number of cells were transferred retro-orbitally in 0.5 mL suspension in PBS under light anesthesia with isoflurane.

For splenocyte accumulation assay, donor splenocytes were isolated from naive B6 or *Ifnar*$^{-/-}$ mice by digesting the spleen with 2.5 mg/mL collagenase D (11088882001, Sigma) at 37°C for 30 min and labeled with 1.0 μM CFSE (eBioscience 65-0580-84, Thermo Fisher) according to the manufacturer's protocol. Ten million cells were transferred into recipient mice that had been treated with DT and immunized as indicated. The left (ndLN) and right (dLN) popliteal LNs were harvested 2 or 72 h after the transfer.

For analyzing the CD4 T cell priming kinetics, CD4 T cells were negatively isolated from the digested spleen and LNs of indicated donor mice with Mouse CD4 T Cell Isolation Kit (STEMCELL Technologies 19852 or BioLegend 480033) according to the manufacturer's protocol and labeled with 1.0 μM CFSE (Thermo Fisher) or CellTrace Violet (C34571, Thermo Fisher). The purity was typically 90-95%. Two million cells were transferred into recipient mice that had been immunized 24 h prior and treated with DT as indicated. In some experiments, multiple types of donor cells (1 x 10^6 cells each) were co-transferred into one mouse. Two h after the transfer, further LN entry of T cells was blocked by retro-orbitally injecting 200 μg anti-CD62L mAb (clone Mel-14, BE0021, BioXCell). The left (ndLN) and right (dLN) popliteal LNs were harvested at indicated time-points.

For analyzing the OT-II cell priming in CD207$^+$ DC-depleted mice, CFSE-labeled OT-II cells (1 x 10^5) were adoptively transferred into DT-treated WT or CD207-DTR mice, followed by immunization with OVA and papain in the footpad. The dLNs were harvested on day 7 post-immunization. For analyzing the OT-II cell priming in CD301b$^{\Delta MHCII}$ mice,

CFSE-labeled OT-II cells (2 x 10^6) were adoptively transferred into CD301b$^{\Delta MHCII}$ or control *Mgl2*$^{+/Cre}$;*H2ab1*$^{+/+}$ mice that had been immunized with OVA and papain for 24 h. The dLNs were harvested for analysis 34 h after the transfer.

For analyzing the priming efficiency of CD4 T cells, titrated numbers of OT-II cells (1, 10, 100, 1,000, or 10,000) were mixed with naive polyclonal CD4 T cells so that the total donor cell number is 10,000 and transferred into the indicated recipients that had been immunized 1 day prior. Alternatively, the mice were immunized without OT-II cell transfer for detecting endogenous TCR Vα2$^+$ CD4 T cells. The dLNs were harvested 4 days after the transfer. Some mice were treated with DT on days −1 and +2.

For the analysis of CD4 T cell re-expansion in response to secondary immunization, WT or Mgl2-DTR mice were transferred with OT-II cells (1 x 10^5) and immunized with OVA and papain in the right footpad on day 0. Alternatively, the mice were immunized without OT-II cell transfer for detecting endogenous TCR Vα2$^+$ CD4 T cells. The mice were then treated with DT on day 16, followed by a secondary challenge with OVA and papain in the left footpad on day 17. The right and left popliteal LNs were harvested 3 days after the secondary challenge. Contraction of the primary response was verified before the secondary immunization by counting the number of circulating OT-II cells in a separate group of WT mice that had been immunized side-by-side with the experimental group.

TRITC painting experiments

A 10% stock solution of Tetramethylrhodamine-5- (and-6)-isothiocyanate (TRITC, Thermo Scientific 46112) was prepared in DMSO and diluted 10 times in acetone immediately before use. DT-treated WT B6 or Mgl2-DTR mice were subcutaneously immunized with papain in the flank skin and simultaneously painted with 20 μL of 1% TRITC on the shaved flank skin directly above the immunization site. The dLNs were harvested 24 h after immunization.

T cell priming in FTY720-treated mice

For analyzing the impact of changes in DC localization on CD4 T cell activation, either OT-II or WT polyclonal CD4 T cells (2 x 10^6) were transferred into recipient WT mice that had been immunized with OVA and papain in the footpad and treated intraperitoneally with 2.5 mg/kg FYT720 (S1PR antagonist, Cayman Chemical NC9015405) or vehicle alone (0.5% ethanol in PBS) 24 h prior. One and a half h after the transfer, further LN entry of T cells was blocked by injecting 200 μg anti-CD62L mAb. The right (dLN) popliteal LNs were harvested 1.5 , 9.5 and 17.5 h after the transfer (0, 8 and 16 h after the CD62L blockade).

Cell preparations and flow cytometry

For staining cell surface antigens, LNs were minced and digested with 2.5 mg/ml collagenase D in complete DMEM with 10% FBS at 37°C for 30 min. In the case of spleen, erythrocytes were lysed by briefly suspending cells in ACK lysis buffer. Cells were resuspended in 2 mM EDTA in PBS and stained with cell viability dye (Zombie Aqua or Zombie UV, BioLegend). Cells were then incubated with 10 μg/mL anti-CD16/CD32 (2.4G2, BioLegend) on ice for 10 min to block non-specific antibody binding to Fc receptors

and stained with fluorochrome-conjugated monoclonal antibodies (mAbs) on ice for 20 min. All staining mAbs were prepared in FACS buffer (1% BSA, 2mM EDTA, 0.05% sodium azide in PBS). For detecting T cell-DC conjugates, the minced LNs were gently mushed with a plunger without collagenase digestion and resuspended in PBS without EDTA.

For intracellular cytokine staining, cells were stimulated in a 96-well round-bottom plate with Cell stimulation cocktail containing PMA and ionomycin (eBioscience 00-4970-03, Thermo Fisher) at 37°C for 1 hour, then incubated another 5 hr at 37 C with additional Protein Transport Inhibitor Cocktail (eBioscience 00-4980-03, Thermo Fisher). Cells were then fixed and permeabilized with BD Cytofix/Cytoperm Kit (BD Biosciences) and incubated with anti-cytokine mAbs for 30 min on ice. For staining Nur77 by mAb, cells were fixed and permeabilized with Foxp3 Fixation/Permeabilization Concentrate and Diluent (eBioscience 00-5521-00, Thermo Fisher).

Antibodies and gating strategies used for flowcytometry analyses are shown in Supplementary Table 1 and fig. S10 unless shown in Figures. Flow cytometry was performed on BD LSRII (BD Biosciences) or Attune NxT (Thermo Fisher) and analyzed by FlowJo software (Version 9.3.2 and 10.5.0, BD).

Immunohistochemistry

Axillary and brachial lymph nodes were harvested from WT or DT-treated Mgl2-DTR mice one day after immunization with OVA and papain in the front footpad and frozen in OCT compound (Sakura Finetek). Cryosections 5-7 μm in thickness were cut and fixed in ice-cold acetone, and non-specific binding was blocked by pre-incubating the sections with 2 % normal goat serum in PBS. For staining DC subsets and HEV, fixed sections were first incubated with 5 μg/ml anti-CD301b (clone URA1, Invitrogen), anti-CD207 (clone eBioRMUL.2, Invitrogen), or biotin-conjugated anti-CD11c (clone N418, BioLegend) mAbs. HRP-conjugated goat anti-rat IgG γ chain-specific antibody (Jackson ImmunoResearch) was used to detect the anti-CD301b and anti-CD207 mAbs and HRP-conjugated streptavidin (SA-HRP, Biotium) was used to detect the biotinylated anti-CD11c mAb. The HRP-conjugated secondary antibody and streptavidin were detected by Alexa Fluor 488 Tyramide (Biotium). The sections were then incubated with 2.5 μg/ml anti-PNAd (clone MECA79, Biolegend), followed by HRP-conjugated anti-rat IgM μ chain-specific antibody (Jackson ImmunoResearch) and Alexa Fluor 647 Tyramide (Biotium). For double staining $CD301b^+$ DCs and B cells, the sections stained for CD301b were incubated with 2.5 μg/ml biotinylated CD45R/B220 (clone RA3-6B2, BioLegend), followed by detection with SA-HRP and Alexa Fluor 647 Tyramide. The nuclei were stained with DAPI (BioLegend). For analyzing DC localization in mice treated with FTY720, axillary and brachial lymph nodes were harvested from WT mice that had been immunized with OVA and papain in the front footpad and intraperitoneally treated with 2.5 mg/kg FYT720 one day prior. DC subsets, HEV, B cells, and nuclei were stained as described above. The sections were mounted in Fluoromount G (Diagnostic BioSystems) and analyzed with a BZ-X710 fluorescence microscope (KEYENCE). For measuring the distance from DCs to the nearest HEV, the distance between the centroid of each DC and the outline of the nearest HEV was measured after segmentation of DCs and HEVs using ImageJ (version 2.1.0/1.53c) with

a plugin DiAna (73). All positions of DCs analyzed were confirmed to be outside of the segmented HEVs.

Statistical Analysis

P-values were calculated by two-tailed Student's t test by Prism software (version 7, GraphPad). Differences were defined as statistically significant when P-values were <0.05. Data are presented as mean ± SEM.

Supplementary Material

Refer to Web version on PubMed Central for supplementary material.

Acknowledgments:

We thank Akiko Iwasaki for Mgl2-Cre and Mgl2-DTR mice. We also thank William Gause and George Yap for critical reading of the manuscript and Alejandro Davila-Pagan, Comparative Medicine Resources and the Flow Cytometry Core at Rutgers New Jersey Medical School for technical assistance.

Funding:

This work was supported by NIH grant R01AI132576 and New Jersey Health Foundation grant PC113-21 to Y.K.

References

1. Bousso P, T-cell activation by dendritic cells in the lymph node: lessons from the movies. Nat Rev Immunol 8, 675–684 (2008). [PubMed: 19172690]
2. Catron DM, Itano AA, Pape KA, Mueller DL, Jenkins MK, Visualizing the first 50 hr of the primary immune response to a soluble antigen. Immunity 21, 341–347 (2004). [PubMed: 15357945]
3. Chudnovskiy A, Pasqual G, Victora GD, Studying interactions between dendritic cells and T cells in vivo. Curr Opin Immunol 58, 24–30 (2019). [PubMed: 30884422]
4. Kumar V et al. , A dendritic-cell-stromal axis maintains immune responses in lymph nodes. Immunity 42, 719–730 (2015). [PubMed: 25902483]
5. Moussion C, Girard JP, Dendritic cells control lymphocyte entry to lymph nodes through high endothelial venules. Nature 479, 542–546 (2011). [PubMed: 22080953]
6. Kumamoto Y, Mattei LM, Sellers S, Payne GW, Iwasaki A, CD4+ T cells support cytotoxic T lymphocyte priming by controlling lymph node input. Proc Natl Acad Sci U S A 108, 8749–8754 (2011). [PubMed: 21555577]
7. Eisenbarth SC, Dendritic cell subsets in T cell programming: location dictates function. Nat Rev Immunol 19, 89–103 (2019). [PubMed: 30464294]
8. Kashem SW, Haniffa M, Kaplan DH, Antigen-Presenting Cells in the Skin. Annu Rev Immunol 35, 469–499 (2017). [PubMed: 28226228]
9. Gerner MY, Casey KA, Kastenmuller W, Germain RN, Dendritic cell and antigen dispersal landscapes regulate T cell immunity. J Exp Med 214, 3105–3122 (2017). [PubMed: 28847868]
10. Gerner MY, Torabi-Parizi P, Germain RN, Strategically localized dendritic cells promote rapid T cell responses to lymph-borne particulate antigens. Immunity 42, 172–185 (2015). [PubMed: 25607462]
11. Itano AA et al. , Distinct dendritic cell populations sequentially present antigen to CD4 T cells and stimulate different aspects of cell-mediated immunity. Immunity 19, 47–57 (2003). [PubMed: 12871638]
12. Gao Y et al. , Control of T helper 2 responses by transcription factor IRF4-dependent dendritic cells. Immunity 39, 722–732 (2013). [PubMed: 24076050]

13. Kumamoto Y, Denda-Nagai K, Aida S, Higashi N, Irimura T, MGL2 Dermal dendritic cells are sufficient to initiate contact hypersensitivity in vivo. PLoS One 4, e5619 (2009). [PubMed: 19440334]
14. Kumamoto Y et al. , CD301b(+) dermal dendritic cells drive T helper 2 cell-mediated immunity. Immunity 39, 733–743 (2013). [PubMed: 24076051]
15. Sokol CL, Camire RB, Jones MC, Luster AD, The Chemokine Receptor CCR8 Promotes the Migration of Dendritic Cells into the Lymph Node Parenchyma to Initiate the Allergic Immune Response. Immunity 49, 449–463 e446 (2018). [PubMed: 30170811]
16. Webster B et al. , Regulation of lymph node vascular growth by dendritic cells. J Exp Med 203, 1903–1913 (2006). [PubMed: 16831898]
17. Kumamoto Y, Hirai T, Wong PW, Kaplan DH, Iwasaki A, CD301b+ dendritic cells suppress T follicular helper cells and antibody responses to protein antigens. Elife 5, (2016).
18. Kissenpfennig A et al. , Dynamics and function of Langerhans cells in vivo: dermal dendritic cells colonize lymph node areas distinct from slower migrating Langerhans cells. Immunity 22, 643–654 (2005). [PubMed: 15894281]
19. Bursch LS et al. , Identification of a novel population of Langerin+ dendritic cells. J Exp Med 204, 3147–3156 (2007). [PubMed: 18086865]
20. Ginhoux F et al. , Blood-derived dermal langerin+ dendritic cells survey the skin in the steady state. J Exp Med 204, 3133–3146 (2007). [PubMed: 18086862]
21. Poulin LF et al. , The dermis contains langerin+ dendritic cells that develop and function independently of epidermal Langerhans cells. J Exp Med 204, 3119–3131 (2007). [PubMed: 18086861]
22. Shiow LR et al. , CD69 acts downstream of interferon-alpha/beta to inhibit S1P1 and lymphocyte egress from lymphoid organs. Nature 440, 540–544 (2006). [PubMed: 16525420]
23. Catron DM, Rusch LK, Hataye J, Itano AA, Jenkins MK, CD4+ T cells that enter the draining lymph nodes after antigen injection participate in the primary response and become central-memory cells. J Exp Med 203, 1045–1054 (2006). [PubMed: 16567390]
24. Bradley LM, Watson SR, Swain SL, Entry of naive CD4 T cells into peripheral lymph nodes requires L-selectin. J Exp Med 180, 2401–2406 (1994). [PubMed: 7525854]
25. Fischer UB et al. , MHC class II deprivation impairs CD4 T cell motility and responsiveness to antigen-bearing dendritic cells in vivo. Proc Natl Acad Sci U S A 104, 7181–7186 (2007). [PubMed: 17435166]
26. Mandl JN et al. , Quantification of lymph node transit times reveals differences in antigen surveillance strategies of naive CD4+ and CD8+ T cells. Proc Natl Acad Sci U S A 109, 18036–18041 (2012). [PubMed: 23071319]
27. Tomura M, Itoh K, Kanagawa O, Naive CD4+ T lymphocytes circulate through lymphoid organs to interact with endogenous antigens and upregulate their function. J Immunol 184, 4646–4653 (2010). [PubMed: 20304829]
28. Au-Yeung BB et al. , A sharp T-cell antigen receptor signaling threshold for T-cell proliferation. Proc Natl Acad Sci U S A 111, E3679–3688 (2014). [PubMed: 25136127]
29. Moran AE et al. , T cell receptor signal strength in Treg and iNKT cell development demonstrated by a novel fluorescent reporter mouse. J Exp Med 208, 1279–1289 (2011). [PubMed: 21606508]
30. Zikherman J, Parameswaran R, Weiss A, Endogenous antigen tunes the responsiveness of naive B cells but not T cells. Nature 489, 160–164 (2012). [PubMed: 22902503]
31. Okuyama M et al. , A novel in vivo inducible dendritic cell ablation model in mice. Biochem Biophys Res Commun 397, 559–563 (2010). [PubMed: 20617552]
32. Stoltzfus CR et al. , CytoMAP: A Spatial Analysis Toolbox Reveals Features of Myeloid Cell Organization in Lymphoid Tissues. Cell Rep 31, (2020).
33. Kuan EL et al. , Collecting lymphatic vessel permeability facilitates adipose tissue inflammation and distribution of antigen to lymph node-homing adipose tissue dendritic cells. J Immunol 194, 5200–5210 (2015). [PubMed: 25917096]
34. Giladi A et al. , Dissecting cellular crosstalk by sequencing physically interacting cells. Nat Biotechnol 38, 629–637 (2020). [PubMed: 32152598]

35. Reinhardt RL, Liang HE, Locksley RM, Cytokine-secreting follicular T cells shape the antibody repertoire. Nat Immunol 10, 385–393 (2009). [PubMed: 19252490]
36. Simmons S et al. , High-endothelial cell-derived S1P regulates dendritic cell localization and vascular integrity in the lymph node. Elife 8, (2019).
37. Conley JM, Gallagher MP, Rao A, Berg LJ, Activation of the Tec Kinase ITK Controls Graded IRF4 Expression in Response to Variations in TCR Signal Strength. J Immunol 205, 335–345 (2020). [PubMed: 32493815]
38. Barnden MJ, Allison J, Heath WR, Carbone FR, Defective TCR expression in transgenic mice constructed using cDNA-based alpha- and beta-chain genes under the control of heterologous regulatory elements. Immunol Cell Biol 76, 34–40 (1998). [PubMed: 9553774]
39. Tubo NJ et al. , Single naive CD4+ T cells from a diverse repertoire produce different effector cell types during infection. Cell 153, 785–796 (2013). [PubMed: 23663778]
40. Moon JJ et al. , Naive CD4(+) T cell frequency varies for different epitopes and predicts repertoire diversity and response magnitude. Immunity 27, 203–213 (2007). [PubMed: 17707129]
41. Polonsky M et al. , Induction of CD4 T cell memory by local cellular collectivity. Science 360, (2018).
42. Schwab SR, Cyster JG, Finding a way out: lymphocyte egress from lymphoid organs. Nat Immunol 8, 1295–1301 (2007). [PubMed: 18026082]
43. Girard JP, Moussion C, Forster R, HEVs, lymphatics and homeostatic immune cell trafficking in lymph nodes. Nat Rev Immunol 12, 762–773 (2012). [PubMed: 23018291]
44. Rivera J, Proia RL, Olivera A, The alliance of sphingosine-1-phosphate and its receptors in immunity. Nat Rev Immunol 8, 753–763 (2008). [PubMed: 18787560]
45. Matloubian M et al. , Lymphocyte egress from thymus and peripheral lymphoid organs is dependent on S1P receptor 1. Nature 427, 355–360 (2004). [PubMed: 14737169]
46. Hall JG, Morris B, The immediate effect of antigens on the cell output of a lymph node. Br J Exp Pathol 46, 450–454 (1965). [PubMed: 5825778]
47. Cahill RN, Frost H, Trnka Z, The effects of antigen on the migration of recirculating lymphocytes through single lymph nodes. J Exp Med 143, 870–888 (1976). [PubMed: 1255114]
48. Lee M, Mandl JN, Germain RN, Yates AJ, The race for the prize: T-cell trafficking strategies for optimal surveillance. Blood 120, 1432–1438 (2012). [PubMed: 22773385]
49. Hochweller K et al. , Dendritic cells control T cell tonic signaling required for responsiveness to foreign antigen. Proc Natl Acad Sci U S A 107, 5931–5936 (2010). [PubMed: 20231464]
50. Stefanova I, Dorfman JR, Germain RN, Self-recognition promotes the foreign antigen sensitivity of naive T lymphocytes. Nature 420, 429–434 (2002). [PubMed: 12459785]
51. Murphy TL et al. , Transcriptional Control of Dendritic Cell Development. Annu Rev Immunol 34, 93–119 (2016). [PubMed: 26735697]
52. Tussiwand R et al. , Klf4 expression in conventional dendritic cells is required for T helper 2 cell responses. Immunity 42, 916–928 (2015). [PubMed: 25992862]
53. Williams JW et al. , Transcription factor IRF4 drives dendritic cells to promote Th2 differentiation. Nat Commun 4, 2990 (2013). [PubMed: 24356538]
54. Schlitzer A et al. , IRF4 transcription factor-dependent CD11b+ dendritic cells in human and mouse control mucosal IL-17 cytokine responses. Immunity 38, 970–983 (2013). [PubMed: 23706669]
55. Satpathy AT et al. , Notch2-dependent classical dendritic cells orchestrate intestinal immunity to attaching-and-effacing bacterial pathogens. Nat Immunol 14, 937–948 (2013). [PubMed: 23913046]
56. Persson EK et al. , IRF4 transcription-factor-dependent CD103(+)CD11b(+) dendritic cells drive mucosal T helper 17 cell differentiation. Immunity 38, 958–969 (2013). [PubMed: 23664832]
57. Lewis KL et al. , Notch2 receptor signaling controls functional differentiation of dendritic cells in the spleen and intestine. Immunity 35, 780–791 (2011). [PubMed: 22018469]
58. Vander Lugt B et al. , Transcriptional programming of dendritic cells for enhanced MHC class II antigen presentation. Nat Immunol 15, 161–167 (2014). [PubMed: 24362890]

59. Dudziak D et al. , Differential antigen processing by dendritic cell subsets in vivo. Science 315, 107–111 (2007). [PubMed: 17204652]
60. Edelson BT et al. , Peripheral CD103+ dendritic cells form a unified subset developmentally related to CD8alpha+ conventional dendritic cells. J Exp Med 207, 823–836 (2010). [PubMed: 20351058]
61. Hildner K et al. , Batf3 deficiency reveals a critical role for CD8alpha+ dendritic cells in cytotoxic T cell immunity. Science 322, 1097–1100 (2008). [PubMed: 19008445]
62. Allenspach EJ, Lemos MP, Porrett PM, Turka LA, Laufer TM, Migratory and lymphoid-resident dendritic cells cooperate to efficiently prime naive CD4 T cells. Immunity 29, 795–806 (2008). [PubMed: 18951047]
63. Leal JM et al. , Innate cell microenvironments in lymph nodes shape the generation of T cell responses during type I inflammation. Sci Immunol 6, (2021).
64. Allan RS et al. , Migratory dendritic cells transfer antigen to a lymph node-resident dendritic cell population for efficient CTL priming. Immunity 25, 153–162 (2006). [PubMed: 16860764]
65. Ochiai S et al. , CD326(lo)CD103(lo)CD11b(lo) dermal dendritic cells are activated by thymic stromal lymphopoietin during contact sensitization in mice. J Immunol 193, 2504–2511 (2014). [PubMed: 25057004]
66. Perner C et al. , Substance P Release by Sensory Neurons Triggers Dendritic Cell Migration and Initiates the Type-2 Immune Response to Allergens. Immunity 53, 1063–1077 e1067 (2020). [PubMed: 33098765]
67. Shiba T et al. , TRPA1 and TRPV1 activation is a novel adjuvant effect mechanism in contact hypersensitivity. J Neuroimmunol 207, 66–74 (2009). [PubMed: 19135264]
68. Shiba T et al. , Transient receptor potential ankyrin 1 activation enhances hapten sensitization in a T-helper type 2-driven fluorescein isothiocyanate-induced contact hypersensitivity mouse model. Toxicol Appl Pharmacol 264, 370–376 (2012). [PubMed: 22935519]
69. Bajenoff M, Granjeaud S, Guerder S, The strategy of T cell antigen-presenting cell encounter in antigen-draining lymph nodes revealed by imaging of initial T cell activation. J Exp Med 198, 715–724 (2003). [PubMed: 12953093]
70. Baptista AP et al. , The Chemoattractant Receptor Ebi2 Drives Intranodal Naive CD4(+) T Cell Peripheralization to Promote Effective Adaptive Immunity. Immunity 50, 1188–1201 e1186 (2019). [PubMed: 31053504]
71. Ingulli E, Ulman DR, Lucido MM, Jenkins MK, In situ analysis reveals physical interactions between CD11b+ dendritic cells and antigen-specific CD4 T cells after subcutaneous injection of antigen. J Immunol 169, 2247–2252 (2002). [PubMed: 12193689]
72. Lee HK et al. , Differential roles of migratory and resident DCs in T cell priming after mucosal or skin HSV-1 infection. J Exp Med 206, 359–370 (2009). [PubMed: 19153243]
73. Gilles JF, Dos Santos M, Boudier T, Bolte S, Heck N, DiAna, an ImageJ tool for object-based 3D co-localization and distance analysis. Methods 115, 55–64 (2017). [PubMed: 27890650]
74. Lee EC et al. , A highly efficient Escherichia coli-based chromosome engineering system adapted for recombinogenic targeting and subcloning of BAC DNA. Genomics 73, 56–65 (2001). [PubMed: 11352566]
75. Heffner CS et al. , Supporting conditional mouse mutagenesis with a comprehensive cre characterization resource. Nat Commun 3, 1218 (2012). [PubMed: 23169059]
76. Liu Z et al. , Fate Mapping via Ms4a3-Expression History Traces Monocyte-Derived Cells. Cell 178, 1509–1525 e1519 (2019). [PubMed: 31491389]

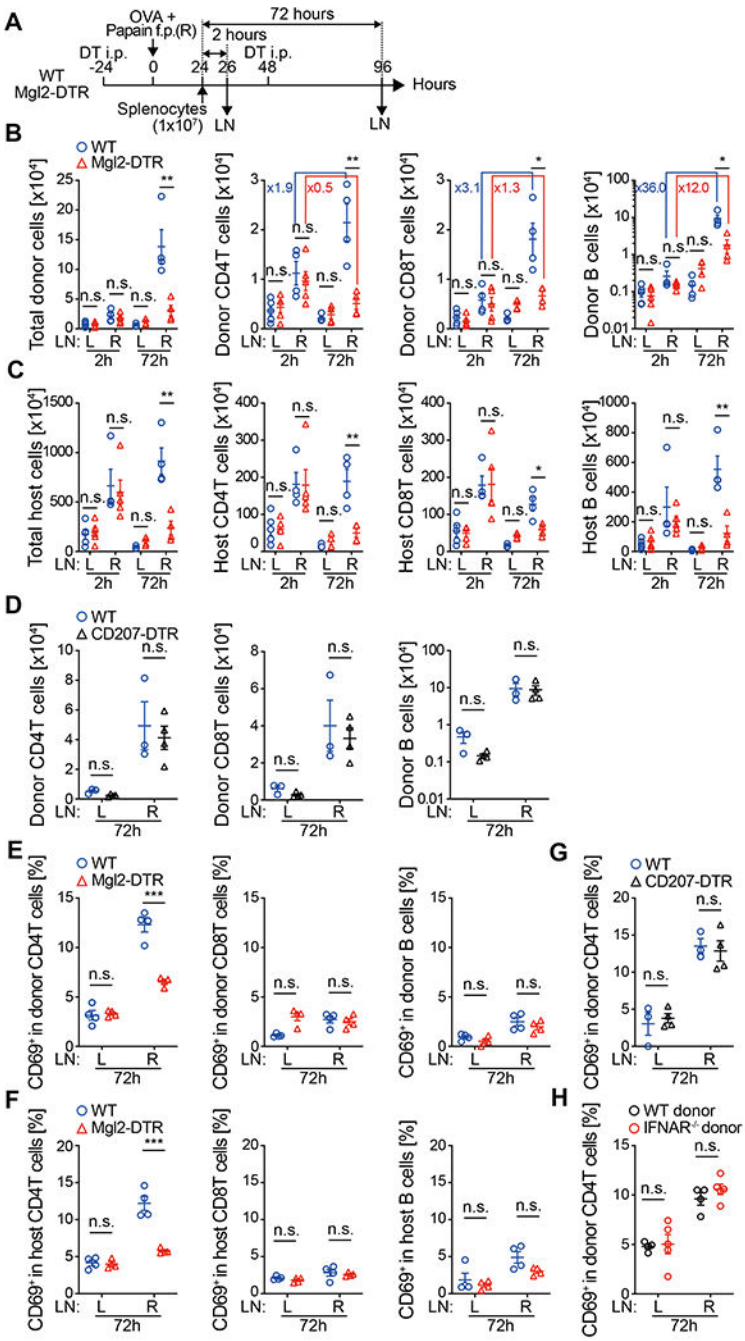

Fig. 1. CD301b$^+$ DCs are required for lymphocyte accumulation and CD69 upregulation in polyclonal CD4 T cells in papain-immunized dLN.

(A) Experimental design. CFSE-labeled splenocytes (1 x 10^7) isolated from naive WT mice were retro-ortbitally transferred into DT-treated WT or Mgl2-DTR mice that had been immunized with OVA and papain in the right hind footpad 24 h earlier. Right draining (R) and left non-draining (L) popliteal LNs were harvested 2 or 72 h after the transfer. **(B and C)** Number of donor **(B)**- and host **(C)**-derived cells recovered from the LNs. **(D)** As in **(A)**, but the cells were transferred into CD207-DTR mice, which were depleted of Langerhans

cells and $CD103^+$ DCs. **(E-H)** Frequency of $CD69^+$ cells in the indicated donor or host cell type 72 h after the adoptive transfer as in **(A)**. Splenocytes of naive WT mice **(E-H)** or $IFNAR^{-/-}$ mice **(H)** were transferred into WT **(E-H)**, Mgl2-DTR **(E and F)**, or CD207-DTR **(G)** recipients. Data represent mean ± SEM of 4-5 (**B**, **C**, **E**, **F**, and **H**) or 3-4 (**D** and **G**) mice per group. n.s., $p \geq 0.05$, *$p < 0.05$, **$p < 0.01$, ***$p < 0.001$, by two-tailed Student's t test.

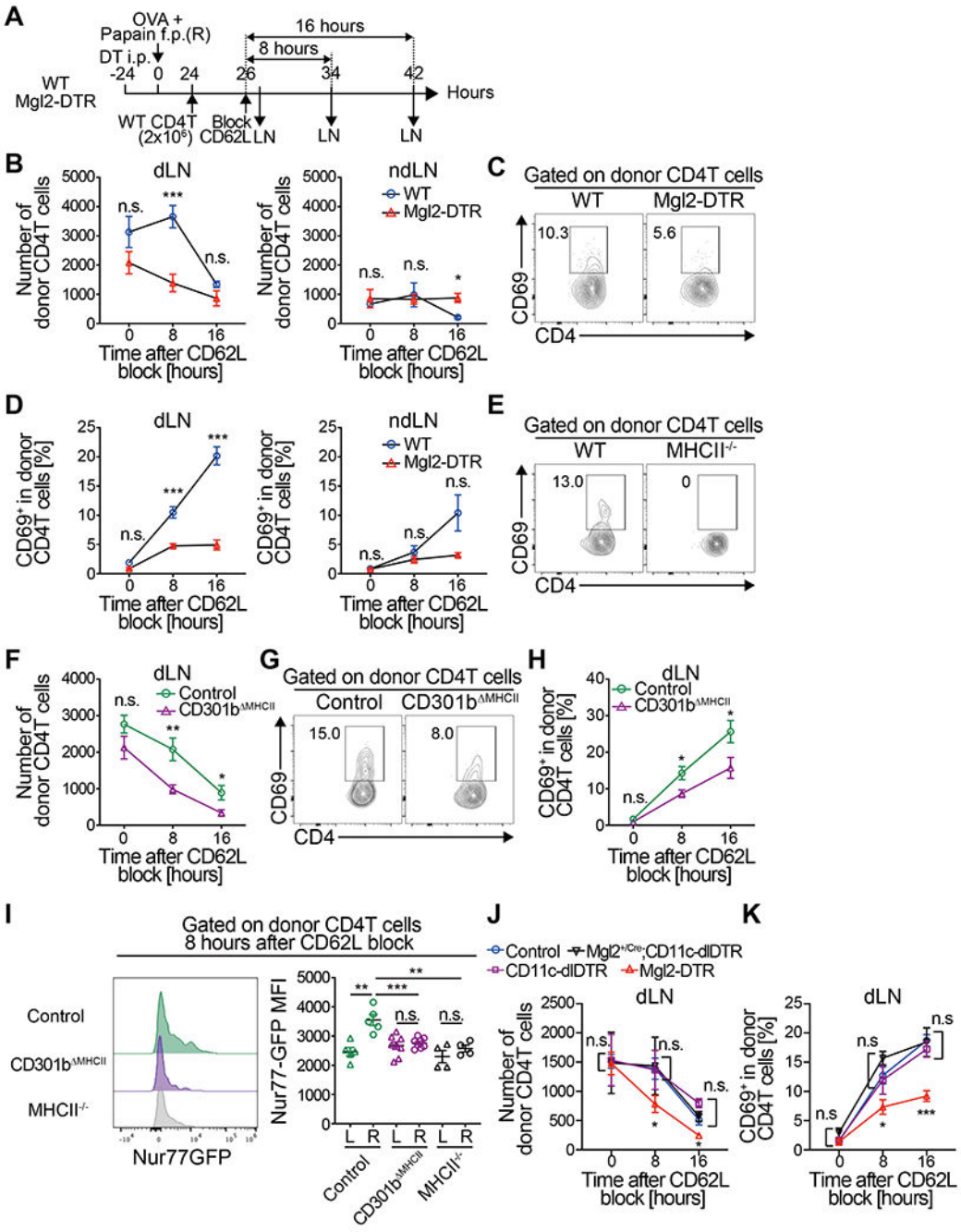

Fig. 2. CD301b^{+} DCs retain and activate naive polyclonal CD4 T cells in the dLN in an MHCII-dependent manner.

(A) Experimental design. Total CD4 T cells were isolated from naive WT donor mice and 2 x 10^{6} cells were transferred into DT-treated Mgl2-DTR or WT mice that had been immunized with OVA and papain in the right footpad 24 h earlier. Two h later, further homing of lymphocytes to LNs was blocked by injecting anti-CD62L mAb. The draining and non-draining popliteal LNs were harvested 0, 8 and 16 h after the CD62L blockade. **(B-D)** Number **(B)** and CD69 expression **(C, D)** of the donor CD4 T cells. **(E-H)** MHCII$^{-/-}$

($H2ab1^{-/-}$) mice **(E)** or $Mgl2^{+/cre}$;$H2ab1^{fl/fl}$ (CD301b$^{\Delta MHCII}$) mice **(F-H)** were transferred with WT CD4 T cells as in **(A)**. $Mgl2^{+/cre}$;$H2ab1^{+/+}$ mice were used as control in **(F-H)**. Number **(F)** and CD69 expression **(E, G, H)** of the donor CD4 T cells are shown. **(I)** Total CD4 T cells isolated from naive Nur77-GFP transgenic mice were transferred into control or CD301b$^{\Delta MHCII}$ mice as in **(A)**. The dLNs (R) and ndLNs (L) were harvested 8 h after the CD62L blockade. Representative FACS histograms (left) and the mean fluorescent intensity (MFI) (right) for the Nur77-GFP reporter expression in the donor CD4 T cells are shown. **(J-K)** Control ($Mgl2^{+/Cre}$), or DT-treated Mgl2-Cre;CD11c-dlDTR, CD11c-dlDTR, or Mgl2-DTR mice were transferred with WT CD4 T cells as in **(A)**. Number **(J)** and CD69 expression **(K)** of the donor CD4 T cells are shown. Data represent mean ± SEM **(B, D, F, H-K)** of 3-9 mice per time-point or representative flow cytometry plot of dLNs 8 h after the CD62L blockade from at least two independent experiments **(C, E, G)**. *$p < 0.05$, **$p < 0.01$, ***$p < 0.001$, n.s., not significant by two-tailed Student's t test.

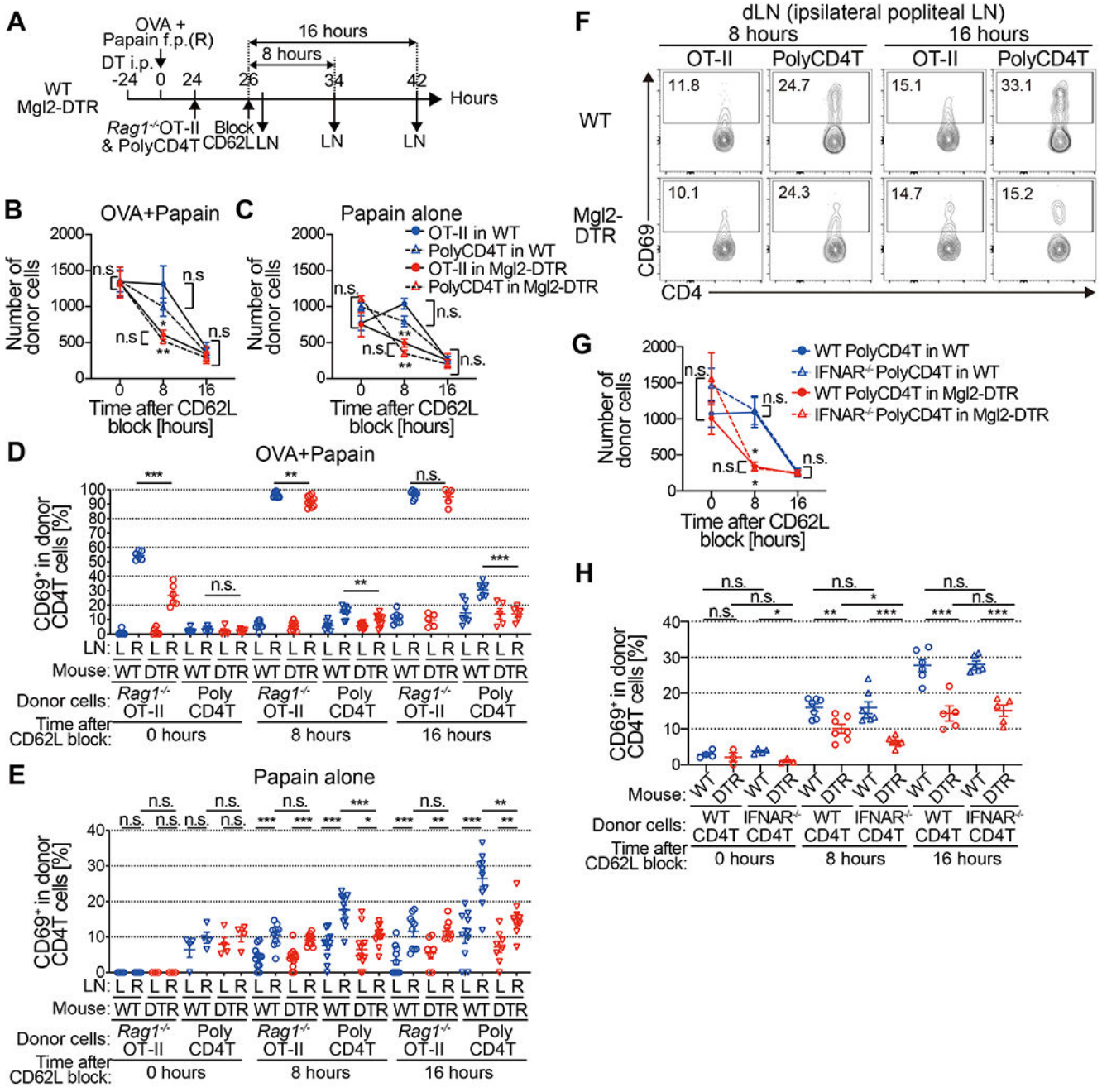

Fig. 3. CD301b^{+} DC-dependent naive CD4 T cell retention in the dLN is independent of TCR specificity.

(A-C) *Rag1*$^{-/-}$ OT-II and WT polyclonal CD4 T cells (1 x 10^{6} cells each) were co-transferred into DT-treated Mgl2-DTR or WT recipients that had been immunized with OVA and papain or papain alone 24 h earlier. The donor cells were allowed to home to LNs for 2 h, after which further homing was blocked with anti-CD62L mAb. The dLN were harvested 0, 8 and 16 h after the CD62L blockade **(A)**. Number of donor CD4 T cells remained in the dLN of mice immunized with OVA and papain **(B)** or papain alone **(C)** at indicated time-points. **(D-F)** *Rag1*$^{-/-}$ OT-II and WT polyclonal CD4 T cells (1 x 10^{6} cells

each) were co-transferred into Mgl2-DTR or WT mice as in **(A)**. Frequency of $CD69^+$ cells in the donor CD4 T cells in mice immunized with OVA and papain **(D)** or papain alone **(E and F)** at indicated time-points. **(G** and **H)** As in **(A)**, but $IFNAR^{-/-}$ and WT polyclonal CD4 T cells (1 x 10^6 cells each) were co-transferred into DT-treated Mgl2-DTR or WT recipients that had been immunized with OVA and papain. Number of donor CD4 T cells remained in the dLN **(G)** and frequency of $CD69^+$ cells in the donor CD4 T cells **(H)** at indicated time-points. *$p < 0.05$, **$p < 0.01$, ***$p < 0.001$, n.s., not significant by two-tailed Student's t test. Pooled data from 4-7 **(B),** 3-6 **(C)** or 3-9 **(G)** mice per group at each time point are shown.

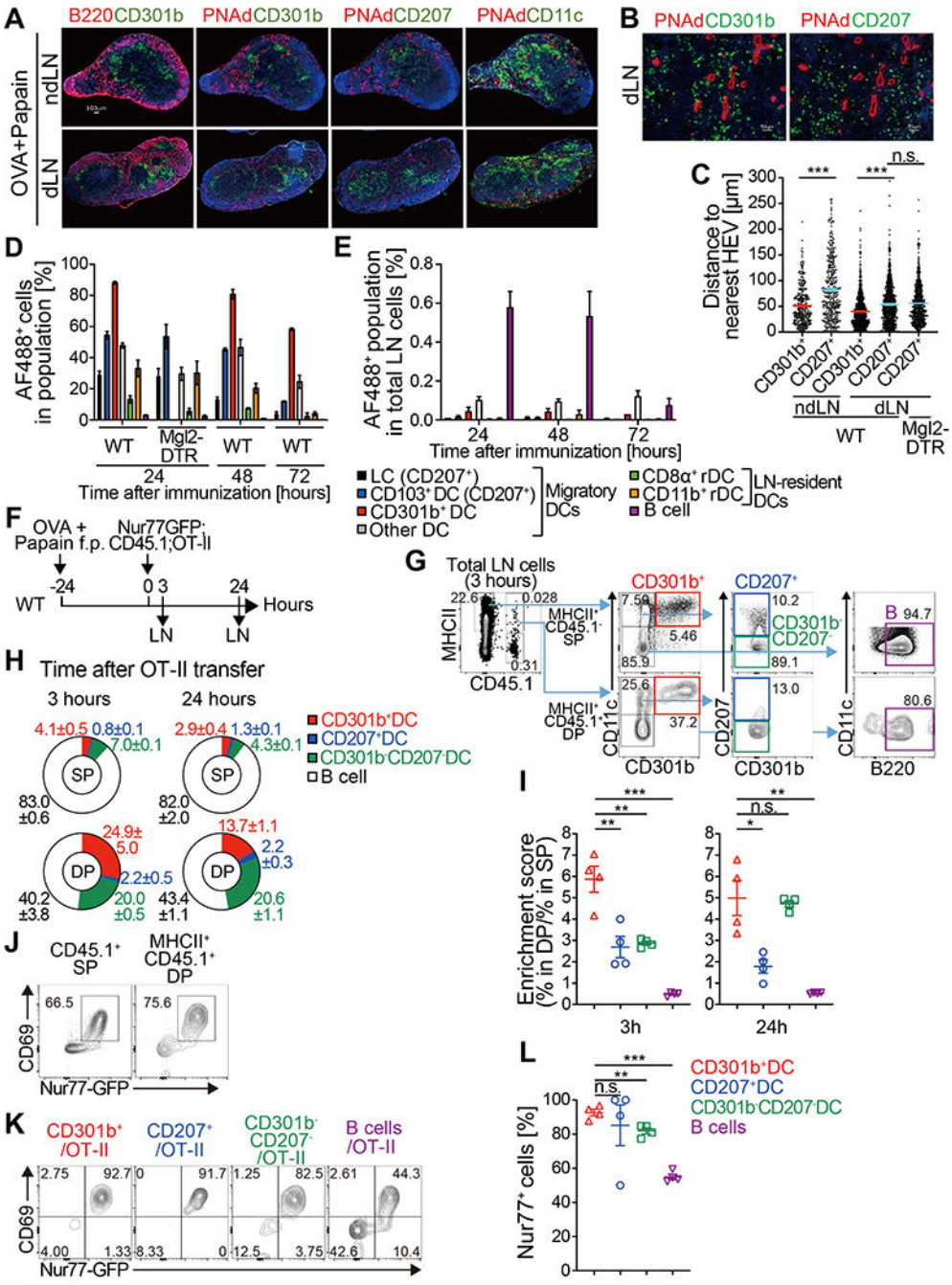

Fig. 4. CD301b$^+$ DCs directly present soluble foreign antigens to CD4 T cells in the dLN immediately after their homing.

(A-C) WT or DT-treated Mgl2-DTR mice were immunized with OVA and papain in the footpad. Twenty-four h later, the dLN and contralateral ndLN were harvested and stained for DC subsets (CD301b, CD207, CD11c), HEV (PNAd) and B cell follicles (B220). Representative images **(A, B)** and the distance of CD301b$^+$ or CD207$^+$ cells to the nearest HEV **(C)** are shown. In (**C**), data are pooled from 2 mice per group and bars represent median values. **(D, E)** WT or DT-treated Mgl2-DTR mice were immunized with Alexa

Fluor 488 (AF488)-labeled OVA protein with papain in the footpad and the dLNs were harvested at indicated time-points. Frequency of $AF488^+$ cells among each cell subset **(D)** and frequency of each $AF488^+$ population among total LN cells **(E)** are shown. LC, Langerhans cell; rDC, LN-resident DC. n=3-4 per each time-point. Data are pooled from two independent experiments and represented as mean ± SEM. **(F-L)** Detection of DC-T cell conjugates ex vivo. Nur77-GFP;CD45.1;OT-II cells (5×10^6 cells) were transferred into WT mice 24 h after immunization with OVA and papain. The dLNs were harvested 3 and 24 h after the transfer and analyzed for the host ($CD45.1^-$) $MHCII^+$ cell-donor OT-II cell ($CD45.1^+$) conjugates by flow cytometry as in **(F)**. Flow cytometric events were analyzed according to the gating strategy for DC and B cell subsets shown in **(G)**. **(H)** Composition of the $MHCII^+$ cells ($CD301b^+$ DCs, $CD207^+$ DCs, $CD301b^-$ $CD207^-$ DCs, and $B220^+$ $CD11c^-$ B cells) within the $CD45.1^-$ $MHCII^+$ single-positive (SP) or $CD45.1^+$ $MHCII^+$ double-positive (DP) flow cytometric events in the dLN 3 (left) and 24 h (right) after the OT-II cell transfer into mice immunized with OVA and papain. **(I)** Enrichment of $CD301b^+$ DCs within the host $MHCII^+$ cell-donor OT-II cell conjugates. Enrichment scores were calculated as [% in $CD45.1^+$ $MHCII^+$ DP/% in $MHCII^+$ SP] for each cell type. **(J)** Expression of CD69 and Nur77-GFP reporter in the $CD45.1^+$ $MHCII^-$ SP or $CD45.1^+$ $MHCII^+$ DP events in the dLNs harvested 3 h after the OT-II cell transfer. **(K, L)** Expression of the Nur77-GFP reporter in the OT-II cells conjugated with indicated cell type in the dLN 3 h after the OT-II cell transfer. Data indicate mean ± SEM **(D, E, I, L)** or representative flow cytometry plots of at least two independent experiments **(G, J, K)**. *$p < 0.05$, **$p < 0.01$, ***$p < 0.001$, n.s., not significant by two-tailed Student's t test.

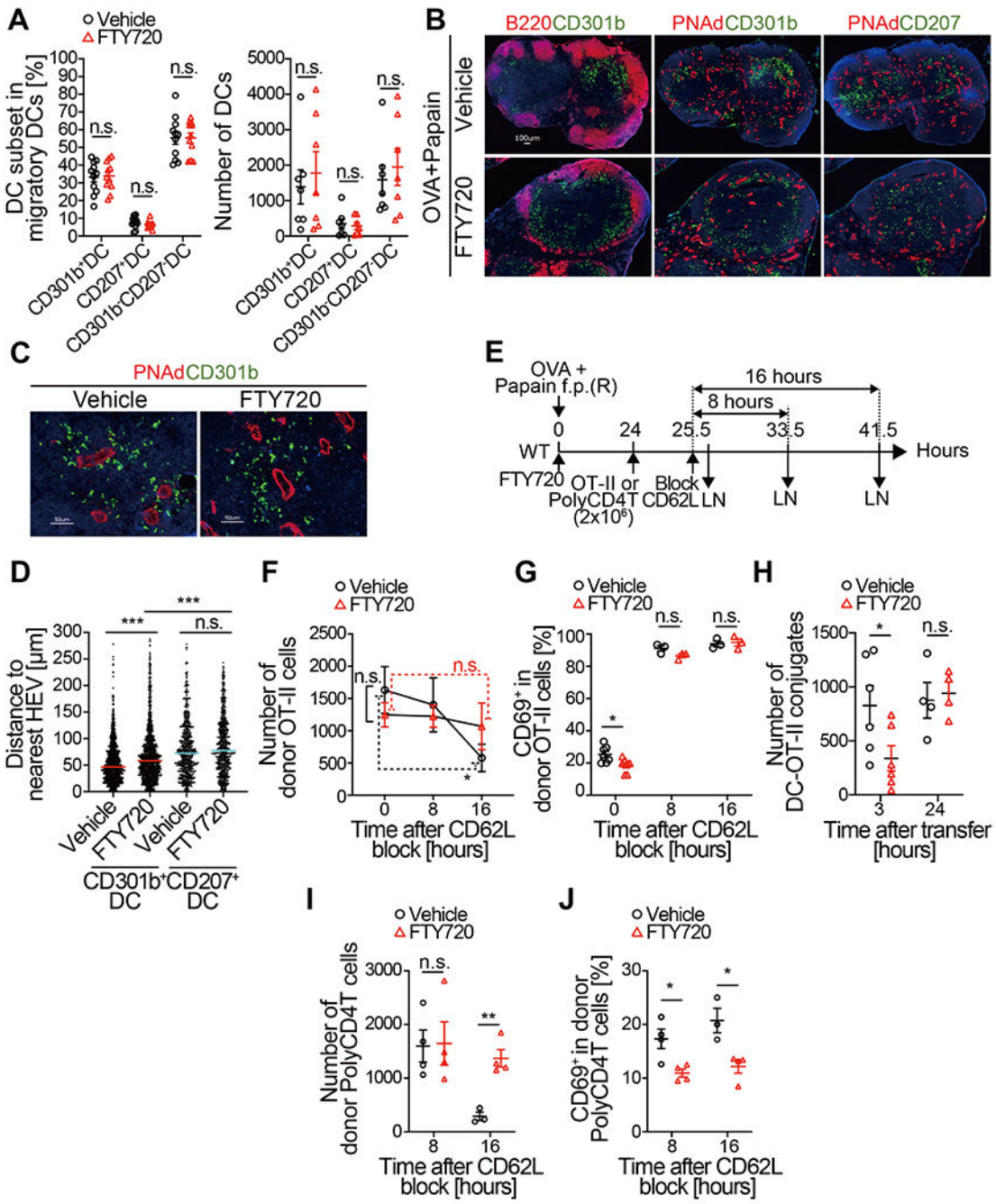

Fig. 5. The positioning of CD301b$^+$ DCs near HEVs facilitates their interaction with incoming naive CD4 T cells.

(A-D) WT mice were immunized with OVA and papain in the footpad and concurrently injected with either FTY720 or vehicle intraperitoneally. Twenty-four h later, the dLNs were harvested and examined for frequencies and localization of DC subsets. **(A)** Frequencies (left) and numbers (right) of DC subsets (CD301b$^+$, CD207$^+$, and CD301b$^-$ CD207$^-$) among total B220$^-$ TCRβ$^-$ Ly6G$^-$ CD11c$^+$ MHCII^{high} migratory DCs are shown. **(B-D)** Representative histological images of DC subsets (CD301b and CD207), HEVs (PNAd),

and B cell follicles (B220) **(B, C)** and the distance of $CD301b^+$ or $CD207^+$ cells to the nearest HEV **(D)** are shown. Bars in **(D)** represent median values. **(E-G)** OT-II cells (2 x 10^6 cells) were transferred into WT mice 24 h after immunization with OVA and papain and injection with either FTY720 or vehicle. The mice were injected with anti-CD62L mAb 1.5 h after the transfer. The draining popliteal LNs were harvested immediately or at indicated time-points after the CD62L blockade. The number **(F)** and the CD69 expression of the donor OT-II **(G)** are shown. **(H)** OT-II cells (5 x10^6 cells) were transferred into WT mice 24 h after immunization with OVA and papain and injection with either FTY720 or vehicle. The dLNs were harvested at indicated time-points and the number of host DC ($CD45.1^-$ $CD11c^+$ $MHCII^+$)-donor OT-II cell ($CD45.1^+$) conjugates was enumerated by flow cytometry. **(I and J)** Same as **(F)** and **(G)** but WT polyclonal CD4 T cells were transferred. Data represent mean ± SEM (A, F-J). *$p < 0.05$, ***$p < 0.001$, n.s., not significant by two-tailed Student's t test.

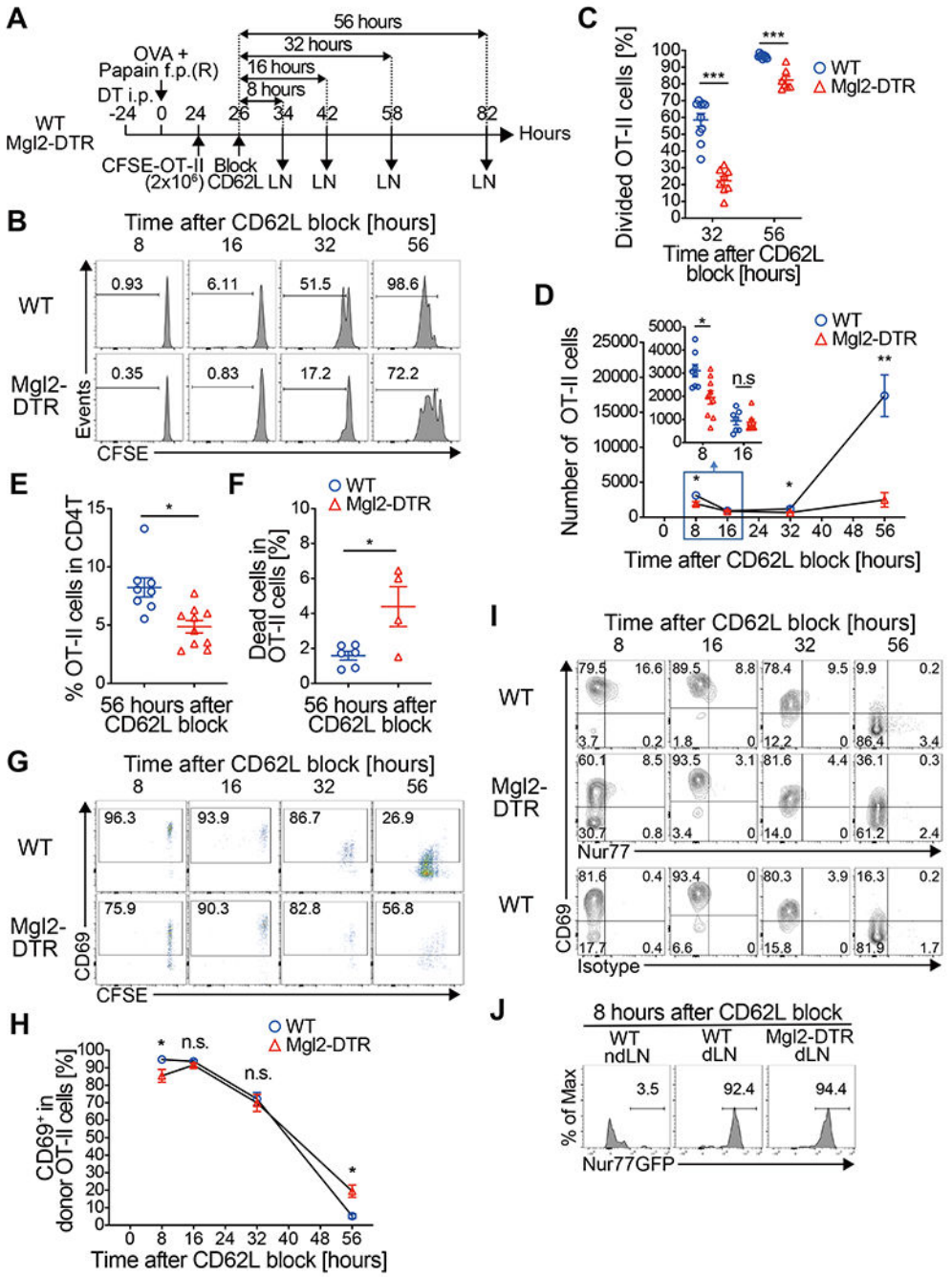

Fig. 6. CD301b$^+$ DCs are required for timely priming of antigen-specific CD4 T cells.

(A-I) CFSE-labeled OT-II cells (2 x 10^6 cells) were transferred into DT-treated Mgl2-DTR or WT mice 24 h after immunization and allowed to home to LNs for 2 h, after which further homing was blocked with anti-CD62L mAb. dLNs were harvested at indicated time-points after the CD62L blockade as in **(A)**. Cell division **(B, C)**, cell numbers **(D)**, percentage among total CD4 T cells **(E)**, cell death **(F)**, CD69 expression **(G, H)** and Nur77 expression **(I)** in the donor OT-II cells at indicated time-points are shown. The inset in **(D)** shows the number of OT-II cells in the dLN 8 and 16 h after the CD62L blockade. **(J)**

Nur77-GFP;CD45.1;OT-II cells (2 x 10^6 cells) were transferred into recipient mice as in **(A)** and the dLNs were harvested 8 h after the CD62L blockade. Nur77-GFP reporter expression of the donor OT-II cells is shown. Data represent mean ± SEM **(C, D, E, F, H)** or show representative flow cytometry plots of at least two independent experiments **(B, G, I, J)**. In **(D)** and **(H)**, data are pooled from 4-9 mice per group at each time-point. *$p < 0.05$, **$p < 0.01$, ***$p < 0.001$, n.s. not significant by two-tailed Student's t test.

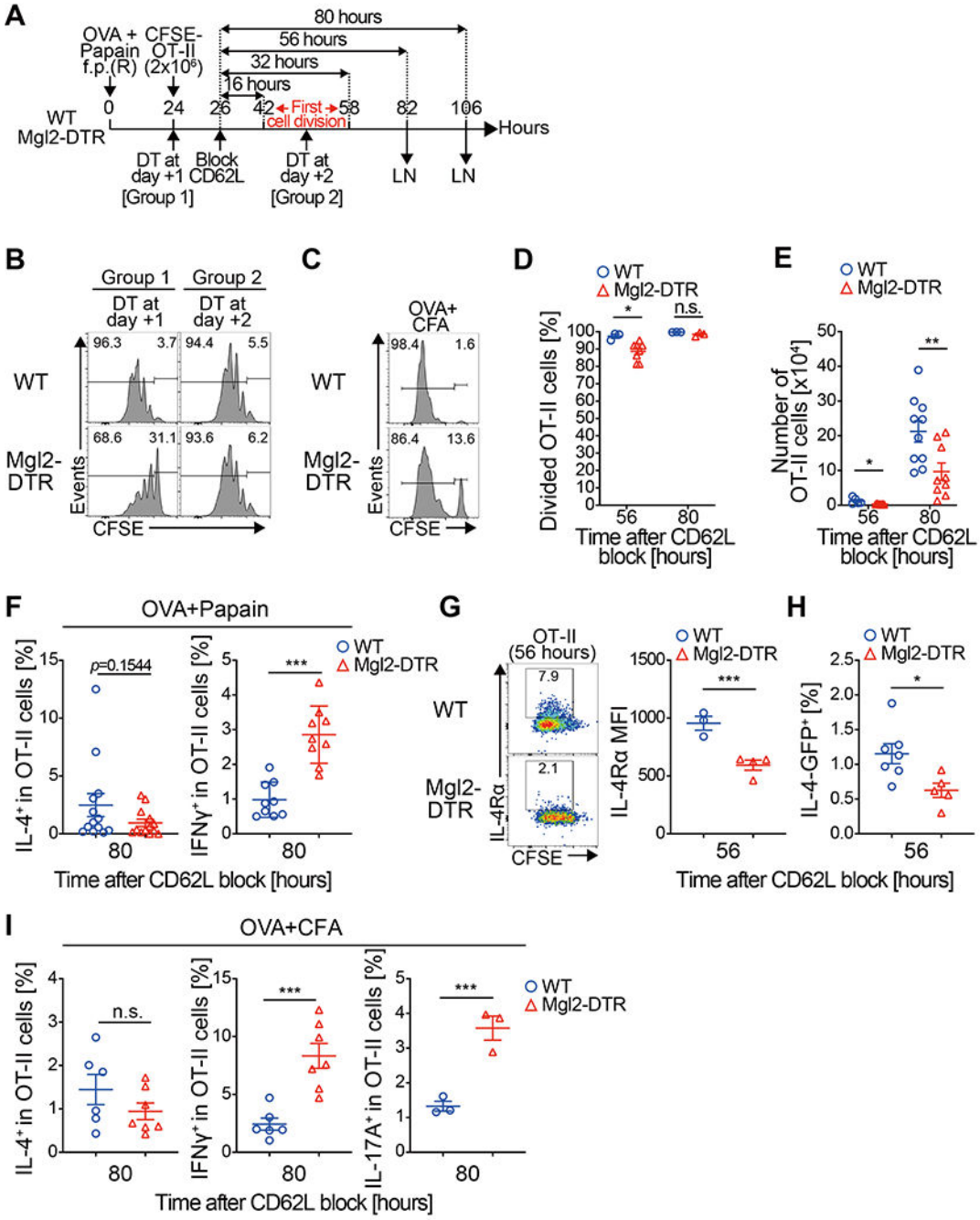

Fig. 7. Early interaction with CD301b$^+$ DCs is critical for the maximal expansion and the fate decision by antigen-specific CD4 T cells.

(A,B) CFSE-labeled OT-II cells (2 x 10^6 cells) were transferred into Mgl2-DTR or WT mice 24 h after immunization with OVA and papain and allowed to home to LNs for 2 h, after which further homing was blocked with anti-CD62L mAb. The recipient mice were treated with DT either 1 or 2 days after the immunization and the dLNs were harvested 56 h after the CD62L blockade as in **(A)**. Cell division profile of the OT-II cells is shown in **(B)**. **(C-E)** CFSE-labeled OT-II cells (2 x 10^6 cells) were transferred into DT-treated Mgl2-DTR or WT

mice 24 h after immunization with OVA and CFA and allowed to home to LNs for 2 h, after which further homing was blocked with anti-CD62L mAb. The dLNs were harvested 56 or 80 h after the CD62L blockade. Cell division **(C, D)**, cell number **(E)** of the OT-II cells in the dLN at indicated time-points are shown. Histograms in **(C)** show representative data at the 56-hour time-point. **(F-I)** OT-II cells (2 x 10^6 cells) were primed with OVA and papain as in Fig. 5A **(F-H)** or with OVA and CFA as in Fig. 6C **(I)**. In **(H)**, 4get;OT-II mice were used as the donor. dLN cells were harvested 80 h after the CD62L blockade and stimulated ex vivo with PMA and ionomycin for intracellular cytokine staining **(F and I)**. Alternatively, the cell surface expression of IL-4Rα or the IL-4-GFP reporter expression in OT-II cells was examined by flow cytometry 56 h after the CD62L blockade **(G and H)**. Frequencies of IL-4^+, IFNγ^+, IL-$17A^+$ or IL-4Rα^+ cells among the donor OT-II cells are shown. Data represent mean ± SEM of 3-10 (**D**, **E**), 9-13 (**F**), 3-4 (**G**), 5-7 (**H**), or 3-7 (**I**) per group **(D-I)** or show representative flow cytometry plot of 3-4 (**B**), 3-8 (**C**), or 3-4 (**G**) mice **(B, C, G)**. *$p < 0.05$, **$p < 0.01$, ***$p < 0.001$, n.s. not significant by two-sided Student's t test.

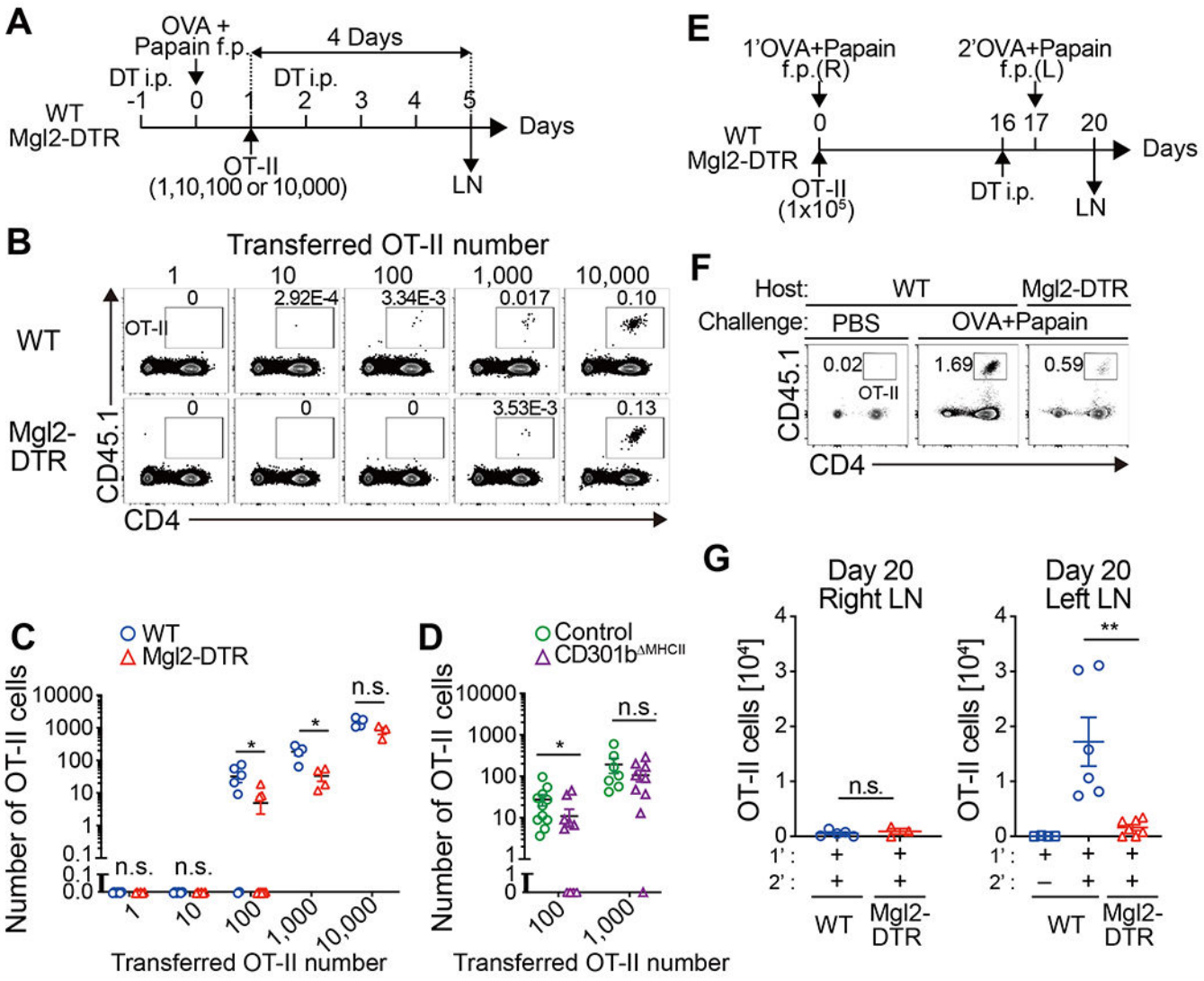

Fig. 8. CD301b^{+} DCs are required for optimal priming and expansion of rare antigen-specific CD4 T cell clones.

(A-C) Titrated numbers (1, 10, 100, 1,000, or 10,000) of CFSE-labeled OT-II cells together with unlabeled WT CD4 T cells (to match the total donor cell number always to 10,000) were transferred into DT-treated Mgl2DTR or WT mice 24 h after immunization with OVA and papain, and the dLNs were harvested 4 days after the adoptive transfer **(A)**. Flow cytometric plots of the total LN cells **(B)** and the number of OT-II cells detected in the dLN **(C)** are shown. Data are pooled from 3–6 mice per group. **(D)** CFSE-labeled naive OT-II cells (100, or 1,000) together with unlabeled WT CD4 T cells were transferred into control or CD301b$^{\Delta MHCII}$ mice 24 h after immunization with OVA and papain. The number of OT-II cells detected in the dLNs 4 days after the immunization is shown. Data pooled from 7-11 mice per group. **(E-G)** WT or Mgl2-DTR mice were transferred with 1 x 10^5 OT-II cells and immunized with OVA and papain in the right footpad on day 0. The mice were treated with DT on day 16 and re-challenged with OVA and papain in the left footpad on day 17. Popliteal LNs were harvested on day 20, 3 days after the secondary challenge **(E)**. Flow

cytometry plots of the total dLN cells in the left popliteal LNs **(F)** and the number of OT-II cells detected in the right (R) or left (L) popliteal LNs are shown. Data represent means ± SEM **(C, D, G)** or show representative flow cytometry plots of at least two independent experiments **(B, F)**. *$p < 0.05$, n.s., not significant, by two-tailed Student's t test.